INSTITUTE FOR SPACE STUDIES

FURTHER STUDIES OF
A NON-LINEAR THERMO-MECHANICAL OSCILLATOR

N. H. Baker
D. W. Moore
E. A. Spiegel

GODDARD SPACE FLIGHT CENTER
NATIONAL AERONAUTICS AND SPACE ADMINISTRATION

FURTHER STUDIES OF A NON-LINEAR THERMO-MECHANICAL OSCILLATOR

N. H. Baker

Columbia University

D. W. Moore

Institute for Space Studies‡

E. A. Spiegel

New York University

‡Now at Imperial College, London

ABSTRACT

Periodic solutions of the equation

$$\dddot{z} + \ddot{z} + (T - R + Rz^2)\dot{z} + Tz = 0$$

are studied numerically and, for large R and T, analytically. The periodic solutions are unstable in a small strip of the (R,T) plane whose boundaries are determined.

§ 1. Introduction

In a recent paper (MOORE and SPIEGEL, 1966, henceforth referred to as MS) a thermo-mechanical oscillator was constructed with the idea of studying, in a simplified system, the properties of non-linear overstability. A small buoyant element was allowed to move in a temperature-stratified fluid under the action of a linear restoring force. The buoyancy of the element was made to depend in a linear way on its temperature which in turn depended on the temperature of the surrounding fluid through Newton's law of cooling. The fact that a finite time is needed for temperature adjustment is essential to the functioning of the model.

This cooling time provides a suitable time scale and if time is measured in these units and if a temperature stratification is chosen so that the surrounding fluid is unstable for $|z| < 1$ and stable for $|z| > 1$ (a cubic law is the simplest analytic function satisfying these requirements and this was used) the equation satisfied by the position $z(t)$ of the small element is

$$\frac{d^3z}{dt^3} + \frac{d^2z}{dt^2} + (T - R + Rz^2)\frac{dz}{dt} + Tz = 0. \quad (1.1)$$

R and T are large when the thermal dissipation involved in the cooling law is small. They can be thought of as the square of the ratio of the cooling time to the characteristic convective time in the absence of the spring and the square of the ratio of the cooling time to the period of free oscillations under the action of the spring alone.

Since energy is available to the small element only for $|z| < 1$ we would expect the motions to be bounded, whatever the initial conditions. Moreover, since the system is dissipative we would expect the system to enter a limit cycle for large values of t . In MS equation (1.1) was studied by time integration and it was found that, while a limit cycle was usually entered, there was a narrow strip of the (R,T) plane in which solutions were not asymptotically periodic. This strip is shown in Figure 1. The purpose of the present paper is to explain the existence of this strip.

In MS it was suggested that the aperiodicity was due to the fact that when R and T lay in the aperiodicity strip the corresponding periodic solutions of (1.1) passed close to the singular point of (1.1) in its phase

$(z, \frac{dz}{dt}, \frac{d^2z}{dt^2})$ space, enabling small numerical errors to push the phase point from one periodic solution to another. (Though the vacillation is induced by numerical errors, the same effect is produced on the actual physical system by small random disturbances. Thus the vacillation is a real physical effect. A rigid simple pendulum with just enough energy to make complete revolutions and subject to small random forces would display a similar vacillation.) Evidence was presented to support this theory of the origin of the vacillation and in particular a few periodic solutions of the required type were discovered using a relaxation procedure.

In this paper a systematic search for the periodic solutions is made. In § 2. an analytic approximation to the periodic solutions of (1.1) is developed which is valid when R and T are very large. In this case the motion is approximately adiabatic and satisfies the energy equation

$$\frac{1}{2R}\left(\frac{dz}{dt}\right)^2 - \frac{1}{2}\delta z^2 + \frac{1}{12}z^4 + Bz = E \tag{1.2}$$

where

$$\delta = 1 - T/R \tag{1.3}$$

and where E is the energy and B the buoyancy of the

element relative to the fluid at $z = 0$ -- both are conserved in the absence of dissipation. To each E and B there corresponds a unique energy curve and to each such energy curve (apart from a single critical curve) corresponds a periodic solution. This degeneracy in the adiabatic theory can be removed in a familiar manner by considering the <u>average</u> effect of the dissipation over the periodic solutions supplied by (1.2). This is valid since there are many oscillations per cooling time if $R \gg 1$. If we do this we find (§ 2a.) that

$$\begin{aligned} \frac{dE}{dt} &= F(E,B,\delta) \\ \frac{dB}{dt} &= G(E,B,\delta) \end{aligned} \tag{1.4}$$

where F and G are averages of the dissipative forces over the energy curves defined by (1.2). If F and G both vanish for particular values E_0 and B_0 then integration of (1.2) with E_0 and B_0 inserted will yield an approximation to the periodic solution of (1.1). This approximate theory shows that a pair of distinct periodic solutions exists which pass vanishingly close to the origin in the phase space of (1.1) as $\delta \to \frac{3}{4}$ from below. These solutions have a characteristic 'spiky' appearance with long flat

portions of small slope between the spikes. For $\delta \geq \frac{3}{4}$ they disappear. This is in good agreement with the time integrations which showed that, to very good approximation, the solutions were asymptotically periodic to the left of the line $\delta \sim \frac{3}{4}$ in the (R,T) plane and had aperiodicity of the "jumping" type just to the right.

Numerical solutions of (1.1) at very large values of R and T, such that (R,T) is in the aperiodicity strip have revealed that near the right hand boundary the aperiodicity takes on a rather different form. Rather than a jumping between periodic solutions with different shapes and periods one has a continuous but aperiodic modulation of a single oscillation (see Figures 2 and 3). Characteristic of the modulation is a gradual decrease in the amplitude of excursions on one side of $z = 0$ followed by a sudden jump to a nearly symmetric motion. The time between the sudden jumps is apparently random (at least we can determine no rules from inspection of about twenty time integrations in this region of the (R,T) plane) and it had no systematic dependence on R.

An explanation of this effect in terms of the (E,B) plane is proposed in § 2d. The singular points of (1.4)

turn out to be all unstable if $.75 \geqslant \delta > .62$ and the point (E,B) traverses a limit cycle in the (E,B) plane. Thus instead of an oscillation of constant amplitude one gets a modulation of the amplitude (and shape) of the oscillation as (E,B) goes round its limit cycle, which is traversed in O(1) cooling times. The sudden jump is associated with the singular energy curve of the family (1.2) which separates energy curves of two types. It is conjectured that the aperiodicity of the modulation is also associated with the singular curve.

At finite R and T we can only hope to find the periodic solutions of (1.1) numerically. However, if R and T lie in the aperiodicity strip these periodic solutions are unstable and will not emerge from a time integration.

In § 3a. we describe a relaxation method of finding the periodic solutions which works even when the solution being sought is unstable. We guess the shape of the solution and its period and improve the guesses by substituting them in the equation and calculating corrections. If we were prepared to solve non-linear algebraic equations for the values of the corrections at the grid points into which we divide the period (normalized to unity, so that the physical period

enters the equation as an eigenvalue) we could find the corrections in one step. Instead we assume formally that the corrections are small and solve the resulting linear equations. The process is repeated until the corrections fall below some pre-assigned value.

The solutions found in this way agree well with the results of time integrations in the stable region of the (R,T) plane and with the asymptotic theory for $R \to \infty$. In particular periodic solutions passing close to the origin of the phase space of (1.1) are found near the line $\delta = \frac{3}{4}$.

In Floquet theory one studies the stability of periodic solutions of a non-linear ordinary differential equation by finding out if small perturbations to the solution grow or decay. The similarity to our numerical procedure is obvious and our procedure yields the Floquet multipliers associated with the periodic solution as well as the periodic solution itself. It is found that the periodic solutions lose stability as a critical curve in the (R,T) plane is crossed from right to left and this curve is in good agreement with the right-hand boundary of the aperiodicity strip.

§ 2. The Method of Averaging

2a. The averaged equations.

In this section we take up the problem of finding approximations to the periodic solutions of (1.1) in the case where R and T are large and $R = O(T)$.

We recall from the physical nature of the system described by (1.1) that infinite R and T correspond to no thermal dissipation, so that in this case the system will execute oscillations of constant amplitude. We shall call these adiabatic oscillations. If R and T are large but finite the dynamical time scale $O(R^{-\frac{1}{2}})$ which characterizes the oscillations is very much shorter than the cooling time $O(1)$ which characterizes the dissipative process. Thus during one oscillation the dissipation can produce only a small effect and we can anticipate that the amplitude, degree of asymmetry and phase of the oscillations will change only very gradually. Consequently one can allow for the effect of the dissipative terms by calculating their average over one oscillation (BOGOLIUBOV and MITROPOLSKY 1961, p. 387 ff.)

Let us introduce a new dimensionless time $\tau = R^{\frac{1}{2}} t$,

so that τ measures time in dynamical units. Then (1.1) can be written

$$\frac{d^3z}{d\tau^3} - (\delta - z^2)\frac{dz}{d\tau} = -R^{-1/2}\left(\frac{d^2z}{d\tau^2} + \frac{T}{R}z\right). \tag{2.1}$$

The small dissipative terms are on the right and the adiabatic motions thus satisfy

$$\frac{d^3z}{d\tau^3} - (\delta - z^2)\frac{dz}{d\tau} = 0. \tag{2.2}$$

This equation was discussed in MS. If we integrate it twice we find that

$$\frac{1}{2}\left(\frac{dz}{d\tau}\right)^2 - \frac{1}{2}\delta z^2 + \frac{1}{12}z^4 + Bz = E \tag{2.3}$$

where E and B are constants of integration. Physically, E is the energy and B the buoyancy defect relative to the fluid at $z = 0$ of the oscillating element. The curves of constant E in the $\left(z, \frac{dz}{d\tau}\right)$ phase plane are closed for all B, so that except for a critical curve which enters a saddle point, every curve, and hence every pair of values (E,B), corresponds to a periodic solution of (2.2).

Thus for any value of δ there is a doubly infinite family of adiabatic oscillations and it is up to the dis-

sipative process to decide which members of this family neither gain or lose energy and buoyancy over one cycle. These particular adiabatic oscillations will be our approximation to the periodic solutions of (1.1) for the given value of δ .

We can integrate (2.3) again in terms of Jacobi elliptic functions but let us write the solution of (2.3) in the form

$$z = z_A(\tau+\theta, E, B, \delta) \tag{2.4}$$

where the new constant of integration θ is a phase, and where the subscript '$_A$' is to emphasize that $z_A(\tau)$ is a solution of the adiabatic approximation (2.3).

We have suggested that for large R the effect of the dissipation will be to slowly change the shape of the adiabatic oscillations. To allow for this we regard θ , E and B not as constants but as varying only over many (actually $O(R^{\frac{1}{2}})$) cycles and we try to choose them so that (2.1) is satisfied in an average sense. As a consequence of the time dependence of the constants,

$$\frac{\partial z}{\partial \tau} = \frac{\partial z_A}{\partial \tau} + \frac{\partial z_A}{\partial \theta}\dot{\theta} + \frac{\partial z_A}{\partial E}\dot{E} + \frac{\partial z_A}{\partial B}\dot{B}$$

where a dot denotes $\frac{d}{d\tau}$. Now if we insist that the last three terms vanish for all t we can ensure that

$$\frac{\partial z}{\partial \tau} = \frac{\partial z_A}{\partial \tau}$$

and by a similar restriction on the second derivatives we can ensure that

$$\frac{\partial^2 z}{\partial \tau^2} = \frac{\partial^2 z_A}{\partial \tau^2}$$

and so

$$\frac{\partial^3 z}{\partial \tau^3} = \frac{\partial^3 z_A}{\partial \tau^3} + \frac{\partial^3 z_A}{\partial \tau^2 \partial \theta}\dot{\theta} + \frac{\partial^3 z_A}{\partial \tau^2 \partial E}\dot{E} + \frac{\partial^3 z_A}{\partial \tau^2 \partial B}\dot{B}$$

Thus we have

$$\left.\begin{aligned} &\frac{\partial z_A}{\partial \theta}\dot{\theta} + \frac{\partial z_A}{\partial E}\dot{E} + \frac{\partial z_A}{\partial B}\dot{B} = 0 \\ &\frac{\partial^2 z_A}{\partial \tau \partial \theta}\dot{\theta} + \frac{\partial^2 z_A}{\partial \tau \partial E}\dot{E} + \frac{\partial^2 z_A}{\partial \tau \partial B}\dot{B} = 0 \\ &\frac{\partial^3 z_A}{\partial \tau^2 \partial \theta}\dot{\theta} + \frac{\partial^3 z_A}{\partial \tau^2 \partial E}\dot{E} + \frac{\partial^3 z_A}{\partial \tau^2 \partial B}\dot{B} = -R^{-1/2}\left(\frac{\partial^2 z_A}{\partial \tau^2} + \frac{T}{R} z_A\right) \end{aligned}\right\} \quad (2.5)$$

where the final equation of the set is derived by insisting that $z(\tau)$ satisfies the full equation (2.1).

The second and third derivatives of z_A in (2.5) can easily be expressed in terms of the first derivatives by using (2.3). For example, if we differentiate (2.3) with respect to E we find

$$\frac{\partial^2 z_A}{\partial \tau \partial E}\frac{\partial z_A}{\partial \tau} = 1 - \frac{\partial z_A}{\partial E}\left(-\delta z_A + \tfrac{1}{3} z_A^3 + B\right)$$

and using this and similar easily derived relations we can show that the solution of (2.5) is

$$\left.\begin{aligned} R^{1/2}\dot{\theta} &= -\left(\frac{\tau}{R} z_A + \frac{\partial^2 z_A}{\partial \tau^2}\right)\left(z_A \frac{\partial z_A}{\partial E} + \frac{\partial z_A}{\partial B}\right) \Big/ \frac{\partial z_A}{\partial \tau} \\ R^{1/2}\dot{E} &= -z_A B + z_A^2 - \tfrac{1}{3} z_A^4 \\ R^{1/2}\dot{B} &= -B + z_A - \tfrac{1}{3} z_A^3 \end{aligned}\right\} \quad (2.6)$$

So far the analysis is exact and we could in principle solve these equations for θ, E, B using the explicit solution (2.4). Needless to say, this is impossible and we replace the right-hand sides in (2.6) by their average values over one oscillation. Let us denote this average

by an overbar. Now

$$\frac{d^2 z_A}{d\tau^2} - \delta z_A + \frac{z_A^3}{3} + B = 0$$

and for a periodic solution

$$\overline{\frac{d^2 z_A}{d\tau^2}} = 0$$

so that, on taking the averages of the right-hand sides of (2.6), we can simplify the equations to

$$\left.\begin{aligned} R^{1/2}\dot{\theta} &= -\overline{\left(\frac{T}{R} z_A + \frac{\partial^2 z_A}{\partial \tau^2}\right)\left(z_A \frac{\partial z_A}{\partial E} + \frac{\partial z_A}{\partial B}\right) \Big/ \frac{\partial z_A}{\partial \tau}} \\ R^{1/2}\dot{E} &= -\overline{z_A B + z_A^2 - \frac{1}{3} z_A^4} \\ R^{1/2}\dot{B} &= \frac{T}{R}\overline{z_A}\,. \end{aligned}\right\} \quad (2.7)$$

These equations are considerably simpler in that there is no explicit time dependence and a solution is feasible. In particular we observe that since the average value of a power of z_A is independent of θ, the last two equations suffice to determine $E(\tau)$ and $B(\tau)$. Thus the phase drops out of the problem (a reflection of the fact

that our system is unforced) and we are left with the pair of equations

$$\left.\begin{aligned} R^{1/2}\dot{E} &= F(E,B,\delta) \\ R^{1/2}\dot{B} &= G(E,B,\delta) \end{aligned}\right\} \quad (2.8)$$

where

$$F(E,B,\delta) = \overline{-z_A B + z_A^2 - \tfrac{1}{3} z_A^4} \quad (2.9)$$

and

$$G(E,B,\delta) = \frac{T}{R}\overline{z_A} \quad (2.10)$$

We are interested in values E_o and B_o which make

$$\left.\begin{aligned} F(E_o,B_o,\delta) &= 0 \\ \text{and} \\ G(E_o,B_o,\delta) &= 0 \ . \end{aligned}\right\} \quad (2.11)$$

We can solve (2.11) directly, but it is instructive to note that solutions of (2.11) are singular points of (2.8) in the (E,B) plane. This suggests that the structure of the solutions of (2.8) in the (E,B) plane will be of interest. For example, if the singular point (E_o,B_o) is unstable we

should not expect to find the corresponding adiabatic oscillation in a time integration of (1.1). The idea of discussing the nature of periodic solutions of a differential equation in terms of the phase plane of the adiabatic constants is due to Andronow and Witt (STOKER 1950, p. 153), who examined second-order forced systems.

Suppose that we are close to a singular point so that

$$E = E_o + \tilde{E}$$

$$B = B_o + \tilde{B}$$

then approximately

$$\left.\begin{aligned} \dot{\tilde{E}} &= F_E^{(o)}\tilde{E} + F_B^{(o)}\tilde{B} \\ \dot{\tilde{B}} &= G_E^{(o)}\tilde{E} + G_B^{(o)}\tilde{B} \end{aligned}\right\} \quad (2.12)$$

and the nature of the singular point is decided by the values of the four partial derivatives, unless the determinant

$$F_E^{(o)} G_B^{(o)} - F_B^{(o)} G_E^{(o)} = 0 \quad (2.13)$$

(STOKER 1950, p. 44). When (2.13) is satisfied there is another solution of (2.8) near (E_0, B_0) so that we have a bifurcation. (The superscript means that the partial derivatives are evaluated at (E_0, B_0)).

The discussion of the structure of the (E,B) plane is greatly facilitated by the introduction of a generating function whose existence was pointed out to us by Whitham (1966 Private communication). Let

$$H(E,B,\delta) = \oint \dot{z}_A^2 \, d\tau = \oint \dot{z}_A \, dz \tag{2.14}$$

where the integral is taken around the energy curve defined by E and B. Clearly $H(E,B,\delta)$ is just the area under the energy curve. Whitham shows that F and G can be expressed in terms of H and its derivatives with respect to E and B and a short calculation gives

$$\left.\begin{aligned} F(E,B,\delta) &= -\frac{1}{P}\frac{(1-\delta)}{\delta}\left\{4E\frac{\partial H}{\partial E} + 3B\frac{\partial H}{\partial B} - \left(\frac{3-4\delta}{1-\delta}\right)H\right\} \\ \text{and} \\ G(E,B,\delta) &= -\frac{1}{P}\frac{\partial H}{\partial B}\ , \end{aligned}\right\} \tag{2.15}$$

where

$$P = \frac{\partial H}{\partial E} \tag{2.16}$$

is the period of the adiabatic oscillation. From (2.15) and (2.11)

$$-\frac{1}{P}\frac{\partial H}{\partial B} = \frac{T}{R}\bar{z}_A \,. \tag{2.17}$$

The system of equations (2.11) has one trivial solution which we can dispose of before proceeding. We can verify analytically that

$$\lim_{E\to 0+}\ \lim_{B\to 0}\ \frac{\partial H}{\partial B} = 0$$

$$\lim_{E\to 0}\ \lim_{B\to 0}\ \frac{\partial H}{\partial E} = \infty$$

while

$$H(0,0) \quad \text{is finite.}$$

Thus $E = 0$ and $B = 0$ is a solution of (2.11) for <u>all</u> ε. The corresponding energy curve is the critical figure of eight curve entering the saddle point $(0,0)$ in the $\left(z, \frac{dz}{d\tau}\right)$ plane, so that the only <u>periodic</u> solution with

$E = 0$ and $B = 0$ is $z_A = 0$, that is, no motion at all! This corresponds to the position of unstable equilibrium at $z = 0$ for the original equation (1.1).

We next prove that (2.11) has non-trivial solutions only when $\delta < \frac{3}{4}$. Clearly $H \geq 0$ and, because the energy curves increase in size as E is increased, $\frac{\partial H}{\partial E} > 0$. Now an energy curve with $E = 0$ passes through the origin in the $\left(z, \frac{dz}{d\tau}\right)$ plane. Thus an energy curve with $E < 0$ is either entirely in the region $z > 0$ or entirely in the region $z < 0$. In either case $z_A \neq 0$ so that in view of (2.17)

$$\frac{\partial H}{\partial B} \neq 0 \quad \text{if} \quad E < 0 . \tag{2.18}$$

Thus solutions are possible only if $E \geq 0$ and the condition for a non-trivial solution to be possible follows at once from the form of F given by (2.15).

We stress that we have not proved that <u>periodic</u> solutions of (1.1) are impossible at large R and T if $\delta \geq \frac{3}{4}$ only that, in this range, the periodic solutions are not approximated by periodic solutions of (2.3). This is confirmed by the time integrations, since for $\delta > \frac{3}{4}$ we found that the equation had periodic solutions, but that these

solutions had several maxima and minima per period, whereas periodic solutions of (2.3) have just one maximum and one minimum per period.

A further transformation is useful. Let

$$z = \delta^{\frac{1}{2}} s \ ,$$

$$E^* = E/\delta^2 \ , \qquad (2.19)$$

and

$$B^* = B/\delta^{3/2} \ .$$

Then

$$H = 2\sqrt{2}\,\delta^{3/2} \int_{s_0}^{s_1} \left(E^* - B^* s + \tfrac{1}{2} s^2 - \tfrac{1}{12} s^4\right)^{1/2} ds \qquad (2.20)$$

where s_0 and s_1 correspond to the points in which the energy curve cuts the z axis. We note that H depends on δ only through the factor $\delta^{3/2}$. Thus the curve Γ in the (E^*,B^*) plane on which $\frac{\partial H}{\partial B^*} = 0$ is independent of δ, so that in view of (2.17) G and $\overline{z}_A$ vanish at every point of this curve. In general F will be non zero except at a finite number of points of Γ and as δ changes these points, which are the singular points of (2.8) in the (E^*,B^*) plane will traverse Γ (Figure 7).

The symmetry of H with respect to B^* shows that

$$\frac{\partial H}{\partial B^*} = 0 \quad \text{on} \quad B^* = 0 \quad (E^* > 0)^+ \tag{2.21}$$

so that one branch of Γ is the positive E^* axis. Indeed it is obvious that z_A vanishes on any symmetric energy curve -- physically, the dissipation does not destroy the symmetry of an initially symmetric motion. These symmetric oscillations are simplest to discuss and we consider them in detail in § 2b. and § 2c. We return to the general case in § 2d., where we find that Γ has a branch on which $B^* \neq 0$, giving rise to asymmetric oscillations.

2b. The symmetric oscillations

If $B^* = 0$ the energy curves are symmetric about the $\frac{dz}{d\tau}$ axis. The critical curve now passes through the origin and corresponds to $E^* = 0$; for $E^* > 0$ the energy curves have a single symmetric branch (Figure 4a).

We now easily see that

$$\frac{H}{2\sqrt{2}\,\delta^{3/2}} = \frac{1}{\sqrt{12}} \int_{-S_0}^{S_0} \sqrt{(S_0^2 - S^2)(S^2 + S_2^2)}\, dS$$

and

+ If $E^* < 0$ the energy curve is entirely above or below the z axis and $\frac{\partial H}{\partial B^*} \neq 0$. $H(E^*, B^*)$ is not differentiable at $(0,0)$.

$$\frac{i}{2\sqrt{2}\,\delta^{3/2}}\,\frac{\partial H}{\partial E^*} = \sqrt{3}\int_{-S_0}^{S_0}\frac{dS}{\sqrt{(S_0^2 - S^2)(S^2 + S_2^2)}}$$

where

$$\left.\begin{aligned} S_0^2 &= 3\left[1 + \left(1 + \tfrac{4}{3}E^*\right)^{1/2}\right] \\ \text{and} \\ S_2^2 &= 3\left[\left(1 + \tfrac{4}{3}E^*\right)^{1/2} - 1\right] . \end{aligned}\right\} \qquad (2.22)$$

The integrals are easily evaluated (Byrd and Friedman 1954, p. 45) and we find that the equation

$$4E^*\frac{\partial H}{\partial E^*} = \frac{3 - 4\delta}{1 - \delta}H$$

which will determine the value of E^* corresponding to a steady oscillation is equivalent to

$$\frac{4E^*}{\left(1 + \frac{4}{3}E^*\right)^{1/2}} = \frac{3 - 4\delta}{1 - \delta}\left\{\left(1 + \tfrac{4}{3}E^*\right)^{1/2} - 1 + 2\frac{E(k)}{K(k)}\right\} \qquad (2.23)$$

where

$$k^2 = \tfrac{1}{2}\left[1 + \left(1 + \tfrac{4}{3}E^*\right)^{-1/2}\right] \qquad (2.24)$$

and where, in the standard notation, $E(k)$ and $K(k)$ are complete elliptic integrals. A rather more convenient form

may be obtained by applying the imaginary modulus transformation to E and K and after some manipulation we find

$$\frac{1}{3}\delta\left(1+\frac{4}{3}E^*\right)^{1/2}+1-\delta=\left(1-\frac{4}{3}\delta\right)\Phi\left(\frac{1+\left(1+\frac{4}{3}E^*\right)^{-1/2}}{1-\left(1+\frac{4}{3}E^*\right)^{-1/2}}\right) \qquad (2.25)$$

where

$$\Phi(\omega)=\frac{\int_0^{\pi/2}\left(1+\omega^2\sin^2\theta\right)^{1/2}d\theta}{\int_0^{\pi/2}\left(1+\omega^2\sin^2\theta\right)^{-1/2}d\theta}\,.$$

Clearly as ω increases from 0 to ∞, Φ increases monotonically from 1 to ∞, so that as E^* increases from 0 to ∞, the right-hand side of (2.25) decreases monotonically from ∞ to $1 - 4/3\delta$ (we assume $0 < \delta < 3/4$) whereas the left-hand side increases monotonically from $1 - 2/3\delta$ to ∞. Thus there is a unique $E^* = E_0^*(\delta)$ for which (2.25) is satisfied and the function $E_0^*(\delta)$ is easily found numerically. Once $E_0^*(\delta)$ is determined, s_0 and s_2 can be found in terms of δ from their definitions (2.22) and the oscillation is given by

$$Z_A=\delta^{1/2}s_0\ \mathrm{sn}\left(\frac{s_2\delta^{1/2}\tau}{\sqrt{6}},\frac{i\,s_0}{s_2}\right)$$

and its period P_{SYM} by

$$P_{SYM} = \frac{4\sqrt{6}\,\delta^{-1/2}}{\sqrt{S_0^2 + S_2^2}}\, K\left(\frac{S_0}{\sqrt{S_0^2 + S_2^2}}\right).$$

P_{SYM} is shown as a function of δ in Figure 5 and we note that it increases rapidly as δ approaches the critical value 3/4. This is because as $\delta \to 3/4 -$, $E_0^*(\delta) \to 0 +$, so that the energy curve is tending to merge with the figure-of-eight curve which has infinite period. In fact it can be shown by expanding for small E* that

$$P_{SYM} \sim \frac{8}{\sqrt{3}} \log\left[\frac{1}{(\frac{3}{4} - \delta)^{1/2}}\right] + O(1)$$

as $\delta \to 3/4 -$.

The form of the oscillations for $\delta = 0.748$ is shown in Figure 6. The flat portion of small slope which is developed when δ is near the critical value is due to the slow motion of the particle near the saddle point (0,0) $\left(z_A, \frac{dz_A}{d\tau}\right)$ plane. This corresponds to a close approach to the origin the phase space $\left(z, \frac{dz}{dt}, \frac{d^2z}{dt^2}\right)$ of the original equation (1.1).

The above analysis is restricted to the case $R \gg T$

for which $\delta > 0$. If $\delta < 0$ very similar analysis can be given and it appears that there is again a unique symmetric solution.

The time integrations showed that there was a stable symmetric solution only when $\delta < .54$, approximately. This suggests that the symmetric solution is unstable when

$$.54 < \delta < .75$$

This is confirmed in § 2c. The time integrations showed a stable asymmetric oscillation when δ was slightly greater than .54. We consider this in § 2d.

2c. The stability of the symmetric solution.

We have seen that a symmetric solution exists in the range $-\infty < \delta < 3/4$. In this section we discuss its stability by examining the nature of the singular point $(E_0^*, 0)$ where $E_0^*(\delta)$ is the solution of the transcendental equation (2.25).

It follows from the symmetry of F with respect to B that

$$F_B(E, 0, \delta) = 0 , \qquad (2.26)$$

so that (2.12) assume the form

$$\dot{\tilde{E}} = F_E^{(0)} \tilde{E}$$

$$\dot{\tilde{B}} = G_E^{(0)} \tilde{E} + G_B^{(0)} \tilde{B}$$

and it follows from STOKER 1950, p. 44, that the point $(E_0, 0)$ is

I) a stable node if

$$F_E^{(0)} G_B^{(0)} > 0 \; ; \; F_E^{(0)} + G_B^{(0)} < 0$$

II) an unstable node if

$$F_E^{(0)} G_B^{(0)} > 0 \; ; \; F_E^{(0)} + G_B^{(0)} > 0$$

III) a saddle point if

$$F_E^{(0)} G_B^{(0)} < 0$$

Now it can be shown from the results of § 2b. that

$$F_E(E_0(\delta), 0, \delta) < 0 \qquad (2.27)$$

Thus case II cannot occur and we have a stable node if $G_B^{(0)} < 0$ and a saddle point of $G_B^{(0)} > 0$. If $G_B^{(0)} = 0$ there will be a bifurcation.

We cannot calculate G_B without considering asymmetric

solutions. However, since the departure from symmetry is small, we can use a perturbation method. Thus to calculate the function $G_B(E_0,0,\delta)$ we write

$$z = z_A(\tau + \theta, E_0(\delta), 0, \delta) + y \ . \tag{2.28}$$

and substitute in (2.3), retaining only terms linear in y. Thus we find

$$\ddot{y} - y(\ddot{z}_A/z_A) = -B(\dot{z}_A/z_A)$$

whose solution is

$$y = -B\dot{z}_A \int (z_A/\dot{z}_A^2)dt + D\dot{z}_A \ ,$$

where D is a constant of integration. However the value of D does not alter the average values involved in the calculation of G_B and we set it equal to zero in subsequent work.

Substituting the explicit form of z_A we find, after some algebra, that

$$y = \frac{6B}{\delta}\frac{s_0^2}{(s_0^2+s_2^2)^2}\left\{1 - \frac{s_2^2}{s_0^2} - 2\,sn^2\left(\frac{s_2\delta^{1/2}T}{\sqrt{6}}, \frac{is_0}{s_2}\right)\right\} \tag{2.29}$$

It is now a straightforward matter to calculate $\bar{y}$ and since

to the order of our approximation,

$$BG_B^{(0)} = \frac{T}{R}\bar{y}$$

we find that

$$G_B^{(0)} = \frac{6T}{R\delta}\frac{s_0^2}{(s_0^2+s_2^2)^2}\left[\frac{6}{s_0^2} - \frac{(2s_0^2-12)\delta}{9-12\delta}\right] . \qquad (2.30)$$

Clearly the sign of $G_B^{(0)}$ is decided by the sign of the quantity in the square bracket in (2.30) and substituting for s_0 its definition (2.22) we have

$$G_B^{(0)} \gtrless 0 \quad \text{if} \quad E^*(\delta) \lessgtr \frac{1}{4}\frac{(9-12\delta)}{\delta}$$

From the numerical solution of the transcendental equation (2.25) which defines $E^*(\delta)$ we find

$$G_B^{(0)}(E_0, 0, \delta) \gtrless 0 \quad \text{if} \quad \delta \gtrless .561\cdots ,$$

and we conclude that the symmetric solution is stable only if

$$\delta < .561\cdots .$$

This is in good agreement with the time integrations of (1.1) for large R .

The critical value of δ corresponds to a bifurcation. In the next section we discuss the structure of the (E^*,B^*) plane as a function of δ and we show that a <u>stable</u> asymmetric solution bifurcates from the symmetric solution at the point corresponding to the critical value. This is also in agreement with the results of the time integrations.

2d. The structure of the (E^*,B^*) plane

We have seen that (2.11) have a symmetric solution for $\delta < 3/4$. To complete our discussion we must examine the possibility of solutions with $B^* \neq 0$. In view of the symmetry of the (E^*,B^*) plane with respect to B^* we need consider only positive B^* .

The energy curves (Figure 4) are

$$\frac{1}{2\delta}\left(\frac{ds}{d\tau}\right)^2 + \frac{1}{2}s^2 - \frac{1}{12}s^4 + B^*s = E^* \qquad (2.31)$$

and we must first discuss how these energy curves depend on E^* and B^* . The positions of equilibria satisfy the cubic

$$s^3 - 3s + 3B^* = 0 \qquad (2.32)$$

so that there are three positions of equilibrium if $0 < B^* < 2/3$ and one if $B^* > 2/3$. Moreover in the first case the central position is unstable and the outer positions stable whereas in the second case the sole equilibrium position is stable (these statements are proved in MS). Thus if $B^* > 2/3$ the energy curves are closed ovals, which increase in size as E^* increases from the value $E^*(s_e)$ appropriate to the position of equilibrium s_e. If $B^* < 2/3$ the situation is more complicated. Let $s_e^{(1)}, s_e^{(2)}, s_e^{(3)}$ be the positions of equilibrium where

$$s_e^{(1)} < s_e^{(2)} < s_e^{(3)}$$

so that $s_e^{(1)}$ and $s_e^{(3)}$ are the stable positions. When $B^* = 0$ $s_e^{(1)} = -\sqrt{3}$, $s_e^{(2)} = 0$ and $s_e^{(3)} = +\sqrt{3}$. As B^* increases $s_e^{(1)}$ and $s_e^{(3)}$ decrease and $s_e^{(2)}$ increases until when $B^* = 2/3$ $s_e^{(2)}$ and $s_e^{(3)}$ merge at the value 1 while $s_e^{(1)} \to -2$. In Figure 7 we sketch the curves $E^*(s_e^{(1)})$ (and its continuation $E^*(s_e)$), marked CD, $E^*(s_e^{(3)})$, marked CA, and $E^*(s_e^{(2)})$ marked OA. Suppose we fix $B^* < 2/3$ and increase E^* from $E^*(s_e^{(1)})$ so that we move along a line parallel to the E^* axis. The energy curve

consists first of a single oval surrounding $s_e^{(1)}$ which increases in size as E^* increases. After we cross CA the energy curve has two branches, one surrounding $s_e^{(1)}$ and one surrounding $s_e^{(3)}$. As E^* increases both ovals grow until on the curve OA they merge and enter the unstable point $s_e^{(2)}$. The energy curve is now a single figure-of-eight curve and the motions are non-periodic. This curve is called the separatrix. When E^* increases still further, the energy curve is a single closed curve surrounding the separatrix.

In short, we have a double branched energy curve in the crescent shaped region C A O and a single branched energy curve everywhere else to the right of CD. The arc OA corresponds to the separatrix.

When the energy curve is double branched, the branch surrounding $s_e^{(3)}$ is entirely in the region $s > 0$ so that clearly $\overline{z}_A \neq 0$ on this branch. Thus when the curve is double branched the branch surrounding $s_e^{(1)}$ is the branch on which H is calculated.

The next step in the discussion is to determine the curve Γ on which $\partial H/\partial B^* = 0$. We have already seen that Γ has a branch $B^* = 0$ corresponding to symmetric oscillations. When $B^* > 0$ solutions are sought numerically,

with the results sketched in Figure 7. An asymmetric branch of Γ bifurcates from $B^* = 0$ at the point Q (which was already located in § 2c.) and returns to the symmetric branch at 0, crossing CA at the point P. The dotted portion of Γ is only inferred since, owing to the proximity of Γ to the critical curve OA corresponding to the separatrix, the numerical work becomes very difficult. Fortunately, on the curve CA, $\partial H/\partial B^*$ can be expressed in terms of elementary functions and the point P located exactly, providing a check on the numerical calculations. The closeness of Γ to OA is shown by the fact that A has coordinates (1/4, 2/3) whereas P has coordinates (.24, .6572 ...)

Near 0 an approximate analytic treatment becomes possible and rather lengthy calculations (Appendix A) show that in the sector AOB*

$$\frac{\partial H}{\partial B^*} = 4\sqrt{6}\,\delta^{3/2}\left(\frac{\pi}{4} - B^* \log \frac{1}{(B^{*2} - 2E^*)^{1/4}}\right) + O(B^*) \qquad (2.33)$$

whereas OA itself is

$$B^{*2} = 2E^* \qquad (2.34)$$

so that $\partial H/\partial B^*$ vanishes on the curve

$$B^{*2} = 2E^* + \exp\left(\frac{-\pi\sqrt{3}}{E^{*1/2}}\right) \qquad (2.35)$$

The proximity of the curves Γ and OA is clear from this formula.

Once Γ is determined the point on Γ at which

$$4E^* \frac{\partial H}{\partial E^*} = \frac{3-4\delta}{1-\delta} H$$

can be found. The arrows on Figure 7 show the direction δ increasing. The bifurcation point Q is, as already seen in § 2d., $\delta = .561$, the point P is $\delta = 5/8$ and at O, $\delta = 3/4$. The period P_{ASM} of the asymmetric oscillations increases rapidly as δ increases (Figure 5); the approximate solution given in Appendix A shows that

$$P_{ASM} \sim \pi^2\sqrt{3}/[2(3-4\delta)] \qquad (2.36)$$

in contrast to the logarithmic behavior of P_{SYM}.

For δ just smaller than 3/4 the energy curve is just inside the lower loop of the separatrix. Consequently the phase point spends most of each period near the point $s_e^{(2)}$, traversing the rest of the energy curve in a time of $O(1)$. As a result the oscillations have a spiked appearance, with

long flat portions between the spikes. Thus the asymmetric solutions also correspond to a close approach to the point $(0,0,0)$ in the $(z,\dot{z},\ddot{z})$ phase space of (1.1) when $\delta \to 3/4 -$.

The nature of the singular point (E_0^*,B_0^*) was also determined. On E^*Q , the singular point is a stable node and on QO , it is a saddle point, so that stable symmetric oscillations are possible only if $\delta < .561$. On QPO , it is at first a stable node, then a stable spiral point and then at R , where $\delta = .62$, it becomes an <u>unstable</u> spiral. Thus for $.561 < \delta < .62$ stable asymmetric solutions are possible. In Figure 8a we show the result of an actual time integration when $\delta = 0.6$. The point (E^*,B^*) is spiralling into a stable spiral point as it should.

When $\delta > .62$ all the singular points of the system (2.8) are unstable. This means that there are no possible stable oscillations in this case. If we integrate (2.8) in time E^* and B^* will not tend to a fixed point as $t \to \infty$ and it is plausible to suppose that there will be a limit cycle. This limit cycle cannot surround the saddle point on OQ , so it must surround either the unstable spiral on OR or the point O itself, which, as we saw in § 2a. is always a singular point of (2.8).

If (E^*,B^*) is describing a limit cycle in the (E^*,B^*) plane the oscillation corresponding to E^* and B^* will undergo a periodic modulation of amplitude and shape. The period will be $O(1)$ cooling times and will depend only on δ. Such periodic modulations of a fundamental periodic solution have been observed for forced motion of a system of two degrees of freedom (Hayashi 1964, p. 309). What is novel in our system is

a) the sudden jump in amplitude

b) the irregular nature of the modulation.

The sudden jump is reasonably simple to explain. Suppose that when the limit cycle is surrounding the unstable spiral point on the asymmetric branch of Γ (that is, a point below R) its lower portion crosses OA . If its lower portion crosses OA it is easy to prove that it does so from left to right. Now crossing OA in this direction means going from the crescent shaped region in which the energy curve has two distinct branches to the region where it surrounds the separatrix. Thus as (E^*,B^*) crosses OA on its limit cycle the corresponding energy curve jumps from an oval just inside the larger portion of the separatrix to a dimpled curve surrounding the whole separatrix (Figure 4b).

Thus the amplitude and shape of the oscillation will change in just the manner observed in the time integrations. In particular the phenomenon will not occur for $\delta < .62$, since the asymmetric solution is then stable, as we have already seen. This is in good agreement with the results of the time integrations.

We have not been able to prove that the limit cycle crosses OA. Instead we have verified the conjecture by time integration of (2.8). The results for $\delta = .625$ are shown in Figure 8b. The solution curve appears to be approaching a limit cycle of the conjectured form.

For $\delta > .7$ the limit cycle still crosses OA, but surrounds the point O, being symmetric about the E^* axis. This presumably reflects a change in character of the singular point as it moves along Γ towards O with increasing δ. However we have not been able to compute Γ in this region, so this remains a conjecture.

Finally, we consider the irregular nature of the oscillation. Suppose that a solution curve of (2.8) crosses OA. On that part of the solution curve near the crossing point the energy curve corresponding to (E^*,B^*) is very close to the separatrix. Thus small changes in E^* and B^* can make a large change in H (recall that $\frac{\partial H}{\partial E^*}$ and $\frac{\partial H}{\partial B^*}$ are

infinite on OA). Thus (2.8) is very sensitive to errors in E* and B* and solution curves which start at neighboring points on the left of OA can widely diverge to the right of OA . Suppose we start numerical integration at a point on the limit cycle. After crossing OA the solution curve will be pushed off the limit cycle by the magnified errors. Subsequently it will spiral back toward the limit cycle. Thus it will again encounter OA and suffer a second random deflection. This process will repeat itself indefinitely so that the solution curve will never coincide with the limit cycle.

This does not conflict with the capture property of stable limit cycles since this depends essentially on the fact that there is a unique solution curve through every point of phase space. The magnified errors can be thought of as random external forcing functions acting on the system (2.8) in a narrow region surrounding OA and in this region there can be many solution curves through any point.

The irregular nature of the solution curve was verified by long time integrations of (2.8).

This explanation of the aperiodicity of the modulation depends on the existence of an unstable spiral singular point

of (2.8). As we have seen the asymmetric singular point goes unstable at $\delta = .62$. This is in good agreement with the right-hand boundary of the aperiodicity strip found by time integration.

§ 3. Periodic Solutions and the Aperiodic Range

3a. The periodic solutions for finite R and T.

In the preceding sections it was seen that for very large values of R and T there can exist symmetric periodic solutions of (1.1) so long as $\delta < .75$. These symmetric solutions are stable only in the range $\delta < .561$ and above this critical value an asymmetric solution exists, which itself is stable only in the range $.561 < \delta < .62$. This asymptotic theory thus predicts that in the range $.62 < \delta < .75$ there will be both symmetric and asymmetric solutions, but that neither type will be stable.

It is to be expected that the asymptotic theory will be approximately valid at large but finite R, and the above description accounts qualitatively for a number of the properties of the solutions at R = 100 found by the numerical time integrations in MS. For example, it was found that the symmetric oscillation always occurred for small values of δ, but that the system settled into an asymmetric oscillation when T was made less than about 44($\delta > .56$).

When T became less than 40($\delta > .60$) the oscillation became aperiodic. No periodic solutions were found in the range $40 > T > 25$ ($.60 < \delta < .75$) and the periodic solutions which appeared for $\delta \geq .75$ were of the multiple-peaked, or squegging, sort which cannot be predicted by the asymptotic theory since this type of solution is not exhibited by equation (2.3). Of course it is not possible to be sure, when a stable periodic solution is found, that it is the only one that exists; and unstable periodic solutions of the sort discussed in the preceding sections cannot be found by the straightforward time-integration technique.

In this section we present examples of the symmetric and asymmetric solutions at finite R in their respective unstable ranges. By using special numerical techniques, it is possible not only to exhibit the unstable periodic solutions, but also to show by the application of Floquet theory that they are indeed unstable in an infinitesimal sense. This offers further confirmation that the "aperiodic" behavior discovered in MS is indeed vacillation among several truly unstable periodic solutions, and that the predictions of the asymptotic theory are qualitatively valid at large but finite R.

Our numerical procedure depends upon a relaxation technique, in which it is demanded that the solution be a periodic one. The problem is changed from a one-point boundary (initial value) problem to a two-point boundary

problem with periodic boundary conditions. Thus only periodic solutions can be found (and of course there is no certainty that one has found all of these). The period appears in the role of an eigenvalue.

In order to apply this procedure equation (1.1) was transformed into a system of three first-order equations, and the independent variable was taken to be $x = t/\lambda$, where λ is the (unknown) period. The system thus becomes (with $y_1 = z$)

$$\begin{aligned} \frac{dy_1}{dx} &= y_2 \\ \frac{dy_2}{dx} &= y_3 \\ \frac{dy_3}{dx} &= -[\lambda y_3 + (T-R+Ry_1^2)\lambda^2 y_2 + T\lambda^3 y_1] \end{aligned} \qquad (3.1)$$

with the boundary conditions

$$y_i(0) = y_i(1) \qquad i = 1, 2, 3 . \qquad (3.2)$$

For definiteness, it is also necessary to fix the phase at some point; for example, we normally take

$$y_1(0) = 0. \qquad (3.3)$$

By a numerical procedure described in Appendix B we proceed to solve the system (3.1) subject to the conditions (3.2) and (3.3). One begins with a set of trial "solutions"

$y_i(x)$ and a trial value of λ, which may either be guessed or taken from the solution of some previous case. In a series of iterations the functions and the eigenvalue are systematically corrected until the equations and conditions are fulfilled to high accuracy. The nature of the initial trial functions normally determines which solution, if any, is finally obtained. With experience it becomes relatively easy to obtain quite rapid convergence to the desired solution. The number of iterations required varies considerably, depending upon both the nature of the solution and the goodness of the trial solution. Regular, nearly sinusoidal solutions are very easily obtained, while strongly asymmetric solutions and those with sharp peaks require many iterations with gentle corrections.

In order that the solutions of the difference equations may approximate as closely as possible those of the corresponding differential equations, the number of mesh points in the interval [0,1] of the independent variable was increased until it was determined that the results no longer changed when the number was further increased. It was found that 1000 points is usually a sufficient number. When this point is reached, the error in the solution presumably depends chiefly upon the accumulated round-off error in the arithmetical operations. In order to keep this as small as possible, double-precision floating-point arithmetic was used throughout (i.e., round-off of an individual number

occurs in the sixteenth significant decimal digit). It was possible to use as many as 4000 equally spaced intervals, and in a few difficult cases it proved necessary to go to this number in order to achieve reliable results.

Some of the results obtained with this procedure are reproduced in Figure 9, for R = 100 and various values of δ in the range $.55 \leq \delta \leq .74$. Time integrations for all cases of this figure are shown in MS. Figure 9a shows the single symmetric solution at $\delta = .55$, just before the bifurcation point. At the slightly larger value $\delta = .60$ (Figure 9b) the asymmetric solution has appeared and it is the stable one. Both this asymmetric solution and the symmetric one of Figure 9a agree with those found by time integration in MS. As δ grows the asymmetry becomes more pronounced as seen in Figure 9c, which is the solution at $\delta = .61$, just into the range where the asymmetric solution has also become unstable and aperiodicity appears in the time integrations. Continuing through the unstable range (Figures 9d and 9e), it may be noted that as in the asymptotic theory the flat "wings" in the symmetric solution become more pronounced, while the asymmetric solution gradually turns into a sharp peak followed by a long "stillstand". The period of the latter solution increases rapidly, as predicted by the asymptotic theory. (All the asymmetric oscillations shown here are for $B < 0$; of course the solutions for $B > 0$ exist as well.)

At $\delta = .74$ ($T = 26$) we are nearing the end of the range where solutions exist according to the asymptotic theory, and the predictions of that theory are becoming less reliable. The symmetric solution (Figure 9f) is still very similar to that of the asymptotic theory (§ 2b). We were not able to obtain the asymmetric solution for $\delta > .71$; as the strongly-peaked character of this solution apparent in Figure 9e becomes still more pronounced, the first and second derivatives of the solution function become very large and the numerical computations come to be dominated by the round-off error. Thus we cannot be sure that the asymmetric solution still exists at $\delta = .74$ for $R = 100$. There has also appeared a new type of periodic solution, the double-peaked oscillation shown at the bottom in Figure 9f. This seems to be an extreme case of the squegging behavior seen in MS at still lower values of T. We did not succeed in finding other periodic solutions at $\delta = .74$, such as a 3-peaked oscillation or the asymmetric 2-peaked solution found at $T = 25$ (see the lowest curve in Figure 3 of MS), but it is quite possible that they exist. In any case it appears that there are no stable periodic solutions at $\delta = .74$, as shown by the extensive time integrations previously reported (see Figure 4 of MS).

We succeeded in finding single-peaked symmetric oscillations up to $\delta = .748$. For larger values of δ no single-peaked periodic solutions were ever found, in good agreement

with our expectations on the basis of the asymptotic theory. The single-peaked symmetric solution at $\delta = .748$ and $R = 100$ is shown in Figure 6, contrasted with that calculated from the asymptotic theory. The solution at $R = 100$ has a period about 5% greater than that of the corresponding asymptotic solution and its shape is also somewhat different. The maximum occurs less than one-quarter period after the zero and there is a tendency toward a "stillstand" on the falling part of the curve. The nature of the solutions at $\delta = .748$ is discussed in more detail below (§ 3c.)

The periods of the symmetric and asymmetric solutions at $R = 100$ are compared in Figure 5 with those computed from the asymptotic theory. A study of this figure reveals the following points. The period of the symmetric solution agrees very well with that predicted throughout the entire range, differing slightly only when δ becomes very close to .75, as noted in the preceding paragraph. The point of bifurcation occurs at a very slightly larger value of δ ($\delta \approx .566$ as compared with $\delta \approx .561$ in the asymptotic theory). Just above the bifurcation the period of the asymmetric solution at $R = 100$ is slightly lower than the asymptotic value, but it has become larger by the time $\delta = .625$ (the numerical asymptotic calculations were not carried beyond this point). In Figure 5 the period P_{ASM} given by the approximate formula (2.36) is also shown. The periods at $R = 100$ are consistently

higher than P_{ASM}. In the range $.62 \leq \delta \leq .70$, the period of the asymmetric solution at R = 100 may be closely approximated by the empirical formula $1/P = .495(.738 - \delta)$ as compared with (2.36) which gives $1/P_{ASM} = .468(.750 - \delta)$. At $\delta = .71$, the highest value for which we were able to compute the asymmetric solution, the period appears to be increasing even more rapidly, possibly indicating that the asymmetric solution disappears at a value of δ somewhat below .75. However the solution at $\delta = .71$ was obtained only with some difficulty and the computed period may not be reliable.

The double-peaked solution on the right in Figure 9f was found in the range $.73 < \delta < .75$. The periods of this solution are also indicated in Figure 5.

In addition to the periods, the quantities E* and B* were evaluated for the periodic solutions at R = 100, allowing a comparison with the Γ curves of the asymptotic solution shown in Figure 7. For the symmetric solutions the dependence of E* on δ given by Equation (2.25) was very closely reproduced by the solutions at R = 100. Furthermore the segment QP of the Γ curve for the asymmetric branch agrees very well with that found at R = 100. (For reasons indicated in § 2d we do not have numerical computations of the asymptotic solution along PO; the portion of this segment near O, where the approximate analytic treatment of Appendix A is applicable, is not accessible to our periodic numerical computations, as discussed earlier in this section.)

3b. Stability of the periodic solutions.

There is yet another point at which the numerical calculations can be compared with the theory; namely, we can investigate numerically the stability of the periodic solutions that have been found. This is accomplished by the application of Floquet theory (STOKER 1950, p. 193 ff.)

The problem investigated in this theory is whether, a periodic solution of a non-linear equation having been found, a small perturbation of this solution will remain bounded. Assume that we have found a periodic solution $\begin{bmatrix} y_1(x) \\ y_2(x) \\ y_3(x) \end{bmatrix}$ of the system (3.1) with period λ. Consider now a vector differing only slightly from the above solution: $\begin{bmatrix} y_1 + w_1 \\ y_2 + w_2 \\ y_3 + w_3 \end{bmatrix}$ where $|w_i(x)| \ll |y_i(x)|$. Then it is found that upon neglecting terms of order w_i^2 and higher, the w_i must satisfy a set of 3 linear equations

$$\frac{dw_i}{dx} = f_{ij}(x)\, w_j(x) \qquad i,j = 1,2,3 \qquad (3.4)$$

with periodic coefficients: $f_{ij}(x + \lambda) = f_{ij}(x)$.

It is possible to find a <u>normal fundamental set</u> of solutions $w_j^n(x)$ of (3.4), and all possible solutions of this linear system can be expressed as linear combinations of the $w_j^n(x)$. The solution $\begin{bmatrix} y_1 \\ y_2 \\ y_3 \end{bmatrix}$ of (3.1) is said to be <u>stable</u> if all solutions $w_j(x)$ of (3.4) remain bounded as $x \to \infty$ which

will be true if and only if all the normal solutions w_j^n are bounded.

Now it is shown in Floquet theory that all the normal solutions $w_i^n(x)$ can be expressed in the form

$$w_i^n(x) = e^{\alpha_i x}\, \varphi_i^n(x)$$

where the $\varphi_i^n(x)$ are periodic functions of x with period λ and α_i is given by

$$e^{\alpha_i \lambda} = \sigma_i.$$

The (in general complex) quantities σ_i are the Floquet multipliers and are the eigenvalues of the Floquet matrix $\underset{\sim}{A}$. This matrix is easily evaluated for any given periodic solution; indeed it is closely related to certain matrices which occur naturally in our iteration scheme to find the periodic solution and, once the scheme has converged, the matrix $\underset{\sim}{A}$ is available with little further computation. The way in which $\underset{\sim}{A}$ is obtained is discussed in detail in Appendix B.

It is now clear that the solution $\begin{bmatrix} y_1(x) \\ y_2(x) \\ y_3(x) \end{bmatrix}$ is stable only if the real parts of all the α_i are non-positive, for in that case all solutions of (3.4) will be bounded. Hence, we must evaluate the eigenvalues σ_i of $\underset{\sim}{A}$, and we shall expect the corresponding periodic solution to be stable only if

$|\sigma_i| \leq 1$ for <u>all</u> σ_i. Since it can be shown that one of the eigenvalues must always be equal to unity, it is the other two which must be determined. In practice, we solve numerically the cubic characteristic equation $||\underset{\sim}{A} - \sigma\underset{\sim}{I}|| = 0$, and verify that one of the roots is always equal to unity as a crude check on our procedure.

In Figure 10 the quantity $\alpha = \lambda^{-1} \ln | \sigma_{max} |$, where σ_{max} is the Floquet multiplier having the largest absolute value, is plotted as a function of δ for the symmetric and asymmetric solutions at R = 100. It is seen that the symmetric solution is stable ($\alpha < 0$) for values of δ below the point of bifurcation. For $\delta \gtrsim .556$, the symmetric solution is unstable and the asymmetric solution is now the stable one. This solution remains stable up to $\delta \approx .606$, after which it too becomes unstable. This is in excellent agreement with the results of the time integrations at R = 100 and also agrees satisfactorily with the predictions of the asymptotic theory.

In part of the stable range of the asymmetric solution, $.589 \lesssim \delta \lesssim .604$, the Floquet multipliers are complex, and in this region α is always equal to -0.5. This region is indicated by the dashed part of the curve in Figure 10. The curve corresponding to the asymmetric solution in Figure 10 extends only to $\delta \approx .64$, although the solution was followed to $\delta = .71$.

This is because the Floquet matrix becomes very ill-conditioned at the larger values of δ, and its eigenvalues can no longer be reliably determined numerically, even though the solution found fulfils the difference equations to a sufficient degree of precision.

The quantity α for the double-peaked solution (Figure 9f) whose period is plotted in Figure 5 is also shown in Figure 10. This solution is never stable throughout the range of its existence, although it is similar, but not identical, to another double-peaked solution which is stable in a small range (see §3c). Finally, it will be remarked that the symmetric solution again appears to become stable for $\delta > .745$. This unexpected behavior is also discussed in the following section.

3c. Some properties of the solutions near $\delta = 3/4$.

It was noted from Figure 10 that the single-peaked symmetric solution at R = 100 becomes stable when $\delta \geq .7455$. This was verified by a time integration at $\delta = .748$, a portion of which is shown in Figure 11a. However this is not the only stable solution; with different initial conditions the apparently stable double-peaked solution of Figure 11b was also found. This is the periodic solution found by time integration at $\delta = .750$ and reproduced in Figure 3 of MS. The solution curve is asymmetric, the peaks above the axis being higher than those below. There is also a tendency toward a "stillstand" before crossing the axis from above, but not from below.

The symmetric double-peaked solution of Figure 9f also exists at $\delta = .748$ and is shown in Figure 11c. Its period is slightly less than that of the solution in Figure 11b, and it is, according to the Floquet multipliers, unstable. It was verified that when a time integration is begun with initial conditions corresponding to the solution of Figure 11c, the oscillation starts off looking like this solution and then settles gradually into the stable solution of Figure 11b. We did not succeed in finding the asymmetric double-peaked solution by the numerical method of § 9a because of the proximity of the more easily found symmetric double-peaked solution.

ACKNOWLEDGEMENTS

We would like to thank Dr. R. Sacker for suggesting the application of Floquet theory. We are particularly indebted to Professor G. B. Whitham for his interest and for pointing out to us the existence of the generating function of § 2. This work was partially supported by the National Science Foundation under Grant GP-5568 (N.H.B.), and by the Air Force Office of Scientific Research under Grant 62-386 (E.A.S.).

REFERENCES

Bogoliubov, N. N. and Mitropolsky, Y. A. 1961, "Asymptotic Methods in the theory of non-linear oscillations" (Delhi: Hindustan Publ. Corp.)

Byrd, P. F. and Friedman, M. D. 1954, "A handbook of elliptic integrals for physicists and engineers" (Berlin: Springer)

Hayashi, C. 1964, "Nonlinear oscillations in physical systems" (New York: McGraw-Hill)

Moore, D. W. and Spiegel, E. A. 1966, Ap. J. 143, 871 (Referred to as MS)

Stoker, J. J. 1950, "Nonlinear vibrations in electrical and mechanical systems" (New York: Interscience)

APPENDIX A: Approximate Solution near 0

Let s_0, s_1, s_2, s_3 be the roots in ascending order of the quartic

$$\frac{1}{12} s^4 - \frac{1}{2} s^2 + B^* s - E^* = 0 \qquad (A.1)$$

These roots are the points in which the energy curve cuts the s axis and in the crescent shaped region OAC of Figure 7, they are all real. The branch which intersects the s axis at s_1 and s_2 has $s > 0$ at every point, so that if we are seeking solutions which make $\bar{s} = 0$, we must take our averages on the branch which intersects the s axis at s_0 and s_1. Thus

$$\frac{\partial H}{\partial B^*} = -\sqrt{2}\,\delta^{3/2} \int_{s_0}^{s_1} \frac{s\,ds}{\left(E^* - B^* s + \frac{1}{2} s^2 - \frac{1}{12} s^4\right)^{1/2}} \qquad (A.2)$$

Standard transformations show that

$$\frac{\partial H}{\partial B^*} = -\frac{4\sqrt{6}\,\delta^{3/2} s_0}{\sqrt{(s_3 - s_1)(s_2 - s_0)}} \int_0^{K(k)} \frac{(1 - \alpha_1^2 \operatorname{sn}^2 u)}{(1 - \alpha^2 \operatorname{sn}^2 u)}\,du \,, \qquad (A.3)$$

where

$$\alpha^2 = -\left(\frac{s_1 - s_0}{s_3 - s_1}\right)$$

$$\alpha_1^2 = \frac{s_3}{s_0}\,\alpha^2 \qquad \text{(A.4)}$$

and

$$k^2 = \frac{(s_3 - s_2)(s_1 - s_0)}{(s_3 - s_1)(s_2 - s_0)} \quad .$$

The standard notation for elliptic functions and integrals is used throughout.

When E^* and B^* are small we can solve (A.1) approximately to find

$$\begin{aligned} s_0 &= -\sqrt{6} + B^* \\ s_1 &= B^* - \sqrt{B^{*2} - 2E^*} \\ s_2 &= B^* + \sqrt{B^{*2} - 2E^*} \\ s_3 &= \sqrt{6} + B^* \end{aligned} \qquad \text{(A.5)}$$

The roots s_1 and s_2 coincide when $B^{*2} = 2E^*$, so this is the approximate equation of OA when E^* and B^* are small. Our approximation is valid in the region AOB* so that $B^{*2} > 2E^*$ and the roots are all real.

We can now easily find approximate expressions for α^2 α_1^2 and k^2, using (A.5). In particular

$$k^2 = 1 - \frac{4}{\sqrt{6}}\sqrt{B^{*2} - 2E^*}$$

so that, since B* and E* are small the complementary modulus k', defined by

$$k' = \sqrt{1 - k^2}$$

is small. In this circumstance the integral in (A.3) can be evaluated approximately (Byrd and Friedman 1954, p. 301) and we find

$$\int_0^K \frac{1 - \alpha_1^2 \, sn^2 u}{1 - \alpha^2 \, sn^2 u} \, du = \left(\frac{1 - \alpha_1^2}{1 - \alpha^2}\right) \log\left(\frac{4}{k'}\right) - \left(\frac{\alpha_1^2 - \alpha^2}{\alpha^2 - \alpha^4}\right)\sqrt{-\alpha^2}\,\tan^{-1}\sqrt{-\alpha^2}$$

$$+ \frac{1}{4}\frac{\alpha_1^2}{\alpha^2} k'^2 \log\left(\frac{4}{k'}\right) + O(k'^2).$$

Substitution of the approximate expressions for α^2, α_1^2 and k'^2 gives equation (2.33) of the text. The integrals for H and $\partial H/\partial E^*$ are rather easier to estimate and we will not give the details of the algebra leading to (2.36).

Appendix B. A numerical method to obtain periodic solutions of nonlinear ordinary differential equations.

In this Appendix we describe in detail the numerical procedure used to obtain the periodic solutions discussed in § 3. The method is based on one which is widely used in stellar structure calculations (L. G. Henyey, J. E. Forbes, and N. L. Gould, Astrophys. J. 139, 306 [1964]) and has been put into the form described here with the help of Dr. L. B. Lucy.

Consider the Nth order system

$$\frac{dy_i}{dt} = g_i(y_j) \qquad i, j = 1, 2, \cdots, N. \tag{B.1}$$

We are seeking periodic solutions of this system, namely a set of functions $y_i(t)$ having the property

$$y_i(t+\lambda) = y_i(t) \tag{B.2}$$

for some real λ and all t. As it is inconvenient in numerical work to have a variable interval for the independent variable, we change to a new independent variable $x = t/\lambda$ and then confine our attention to a single period: $0 \le x \le 1$. Our system is now

$$\frac{dy_i}{dx} = f_i(y_j; \lambda) \qquad i, j = 1, 2, \cdots, N \tag{B.3}$$

and the required property (B.2) is expressed as a set of boundary conditions:

$$y_i(1) = y_i(0) \qquad i = 1, 2, \cdots, N. \tag{B.4}$$

The problem now has the character of a two-point boundary problem, with the period λ as an eigenvalue. The conditions (B.4), however, do not suffice to determine a solution of (B.3), since the phase is not fixed; i.e., any solution can be arbitrarily translated in x and remains a solution. Thus we need some (quite arbitrary) condition to define the phase of one particular y_i. Normally we take

$$y_1(0) = C = \text{const.} \tag{B.5}$$

It is important only that the value of the constant lie within the (normally bounded) range assumed by y_1.

In order to construct difference equations, we divide the range [0,1] into M intervals, not necessarily of equal length. Thus there will be M + 1 mesh points, labeled x_1, x_2, $\cdots\cdots x_M$, x_{M+1}, with $x_1 = 0$ and $x_{M+1} = 1$. The interval between two mesh points is then $\Delta x^m = x_{m+1} - x_m$. Values of the y_i, etc. at $x = x_m$ will be denoted by a superscript, thus: $y_i(x_m) = y_i^m$. Using a simple first-order difference scheme, the equations (B.3) between points m and m+1 become

$$\frac{y_i^{m+1} - y_i^m}{\Delta x^m} = \frac{1}{2}\left[f_i(y_j^{m+1}; \lambda) + f_i(y_j^m; \lambda) \right] \tag{B.6}$$

and conditions (B.4) and (B.5) become

$$y_i' = y_i^{M+1} \tag{B.7}$$

and

$$y_1' = C \tag{B.8}$$

respectively.

Our approach will be to find a method of repeatedly correcting a given set of trial functions until we obtain a set which satisfies the equation. To this end, let us assume a set of trial functions $\bar{y}_i(x)$ having values $\bar{y}_i^m$ at the mesh points and a trial eigenvalue $\bar{\lambda}$ (obtained either from an initial guess or from the previous iteration). The $\bar{y}_i^m$ do not satisfy the equations (B.6), but we now seek an improved set

$$y_i^m = \bar{y}_i^m + \delta y_i^m,$$
$$\lambda = \bar{\lambda} + \delta\lambda.$$

Then, with the notations

$$f_i^m = f_i(y_j^m; \lambda) \qquad \bar{f}_i^m = f_i(\bar{y}_j^m; \bar{\lambda})$$
$$f_{ij} = \partial f_i / \partial y_j \qquad f_{i\lambda} = \partial f_i / \partial \lambda$$

we write

$$f_i^m = \bar{f}_i^m + f_{ij}^m \delta y_j^m + f_{i\lambda}^m \delta\lambda + \cdots\cdots\cdots$$

(summation on repeated lower indices, not on repeated upper indices). The difference equations (B.6) are now linearized

by inserting the above expansions and neglecting terms of order δy_i^2 and $\delta\lambda^2$. The result, after some rearrangement, is

$$\left.\begin{aligned}&\left(\tfrac{1}{2}f_{ij}^{m+1}-\frac{1}{\Delta x^m}\delta_{ij}\right)\delta y_j^{m+1}+\left(\tfrac{1}{2}f_{ij}^{m}+\frac{1}{\Delta x^m}\delta_{ij}\right)\delta y_j^{m}\\&+\tfrac{1}{2}\left(f_{i\lambda}^{m+1}+f_{i\lambda}^{m}\right)\delta\lambda=\frac{1}{\Delta x^m}\left(\bar{y}_i^{m+1}-\bar{y}_i^{m}\right)-\tfrac{1}{2}\left(\bar{f}_i^{m+1}+\bar{f}_i^{m}\right),\end{aligned}\right\}\quad(B.9)$$

and the conditions (B.7) and (B.8) become

$$\left.\begin{aligned}&\delta y_i^1-\delta y_i^{M+1}+\left(\bar{y}_i^1-\bar{y}_i^{M+1}\right)=0\\&\delta y_1^1+\left(\bar{y}_1^1-C\right)=0.\end{aligned}\right\}\quad(B.10)$$

Between any two mesh points, then, we must compute the N x N matrices

$$\left.\begin{aligned}&a_{ij}^m=\left[\tfrac{1}{2}f_{ij}^{m+1}-\frac{1}{\Delta x^m}\delta_{ij}\right],\quad b_{ij}^m=\left[\tfrac{1}{2}f_{ij}^{m}+\frac{1}{\Delta x^m}\delta_{ij}\right]\\&\text{and the 1 x N column vectors}\\&c_i^m=\tfrac{1}{2}\left(f_{i\lambda}^{m+1}+f_{i\lambda}^{m}\right),\quad e_i^m=\tfrac{1}{2}\left(\bar{f}_i^{m+1}+\bar{f}_i^{m}\right)-\frac{1}{\Delta x^m}\left(y_i^{m+1}-y_i^{m}\right)\end{aligned}\right\}\quad(B.11)$$

With these definitions, (B.9) becomes

$$a_{ij}^m\,\delta y_j^{m+1}+b_{ij}^m\,\delta y_j^m+c_i^m\,\delta\lambda+e_i^m=0.\quad(B.12)$$

Defining now the inverse $a^{-1}{}_{ij}^{m}$ of a_{ij}^{m}; viz.,

$$a^{-1}{}_{ik}^{m}\, a_{kj}^{m} = \delta_{ij} \tag{B.13}$$

and the quantities .

$$B_{ij}^{m} = -a^{-1}{}_{ik}^{m}\, b_{kj}^{m}, \quad C_i^{m} = -a^{-1}{}_{ik}^{m}\, c_k^{m}, \quad E_i^{m} = -a^{-1}{}_{ik}^{m}\, e_k^{m}, \tag{B.14}$$

one obtains

$$\delta y_i^{m+1} = B_{ij}^{m}\, \delta y_j^{m} + C_i^{m} \delta\lambda + E_i^{m}. \tag{B.15}$$

We now seek a similar relation between the corrections at any given point and those at the first boundary point, thus:

$$\delta y_i^{m+1} = \beta_{ij}^{m}\, \delta y_j^{1} + \gamma_i^{m} \delta\lambda + \varepsilon_i^{m}. \tag{B.16}$$

The β_{ij}^{m}, γ_i^{m}, and ε_i^{m} can be found because, clearly,

$$\beta_{ij}^{1} = B_{ij}^{1}, \quad \gamma_i^{1} = C_i^{1}, \quad \varepsilon_i^{1} = E_i^{1} \tag{B.17}$$

and, combining (B.15) and (B.16) we obtain a set of recurrence relations:

$$\left.\begin{aligned} \beta_{ij}^{m} &= B_{ik}^{m}\, \beta_{kj}^{m-1} \\ \gamma_i^{m} &= B_{ik}^{m}\, \gamma_k^{m-1} + C_i^{m} \\ \varepsilon_i^{m} &= B_{ik}^{m}\, \varepsilon_k^{m-1} + E_i^{m}. \end{aligned}\right\} \tag{B.18}$$

Beginning with (B.17) and applying (B.18) repeatedly, we finally arrive at a relation between the corrections at the two ends of the interval [0,1]:

$$\delta y_i^{M+1} = \beta_{ij}^{M} \delta y_j^{1} + \gamma_i^{M} \delta\lambda + \varepsilon_i^{M} \,. \qquad \text{(B.19)}$$

These constitute N linear equations relating the 2N + 1 quantities δy_i^{M+1}, δy_i^{1}, $\delta\lambda$. In addition, we have the N + 1 relations (B.10) and upon eliminating the δy_i^{M+1} from (B.19) with the first of (B.10), we have N + 1 equations in N + 1 unknowns, which we then solve for the δy_i^{1} and $\delta\lambda$. Applying (B.15) successively at each mesh point, we then obtain all the corrections δy_i^{m} at each point. The corrections are added to the $\bar{y}_i^{m}$ and $\bar{\lambda}$ and the whole procedure is repeated.

It may be mentioned that in difficult cases, and especially when the trial function is poor, it often proves expedient to apply not the full correction, but only a certain fraction, ν , of it. Thus the new functions would be

$$y_i^{m} = \bar{y}_i^{m} + \nu \cdot \delta y_i^{m} \qquad 0 < \nu < 1 \,.$$

After a number of iterations ν may be increased, and when the "solution" becomes so good that the linear approximation (B.9) is quite good, the convergence is speeded by setting $\nu = 1$. In the present calculations it was found that, when convergence was obtained, the largest relative correction

to any variable at any mesh point,

$$\left|\frac{\delta y_i^m}{y_i^m}\right|_{MAX} \approx 10^{-5}$$

as a typical value.

When the procedure has converged, the $y_i(x)$ are periodic functions satisfying (B.6). If now we repeat the process once more, the δy_i are just the $w_i(x)$ of the Floquet theory (cf. Eq. 3.4), and the Floquet matrix $\underset{\sim}{A}$ is evidently just

$$\underset{\sim}{A} = (\beta_{ij}^M),$$

the matrix already calculated for use in Eq. (B.19).

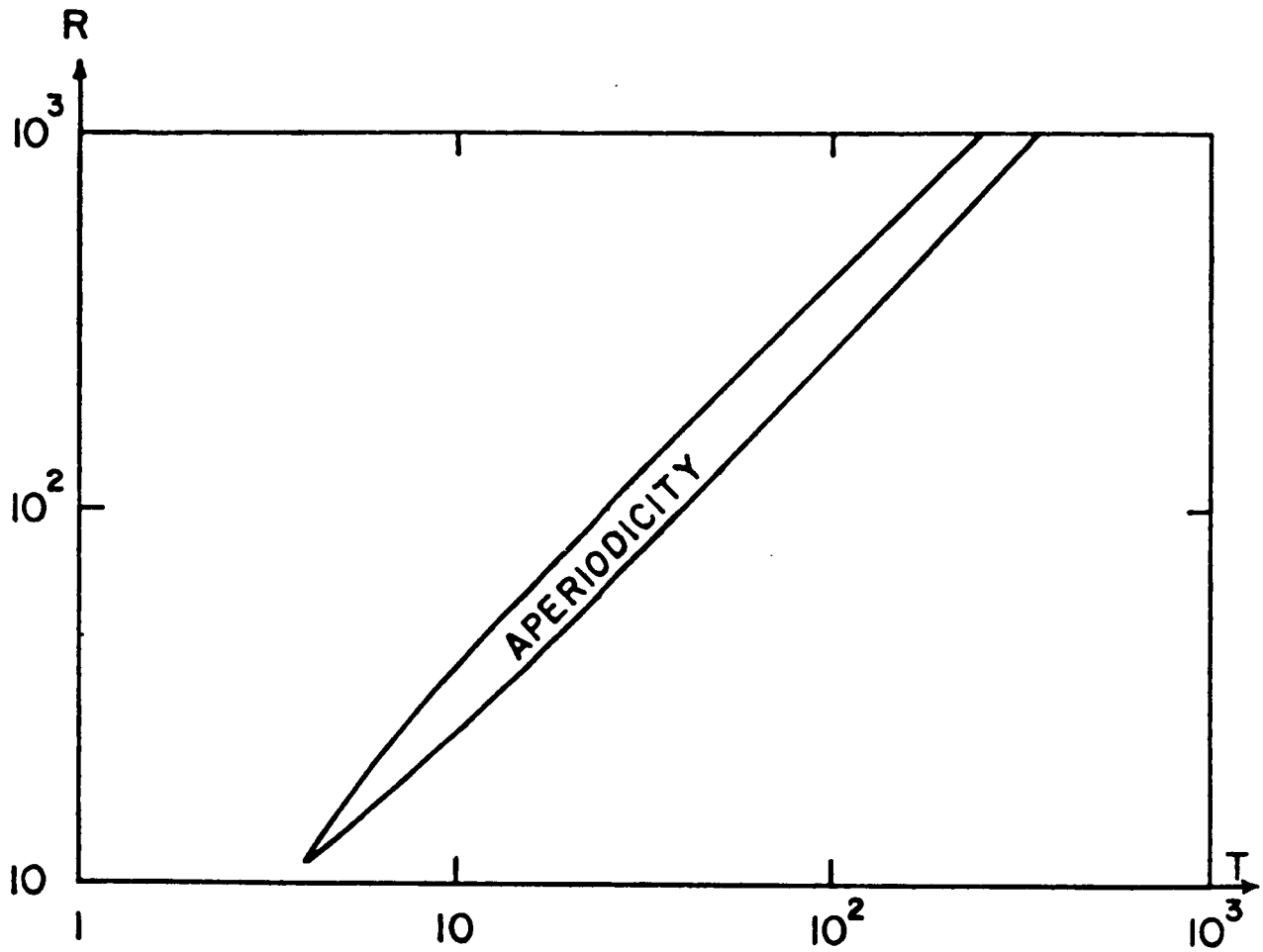

Figure 1. The aperiodicity strip.

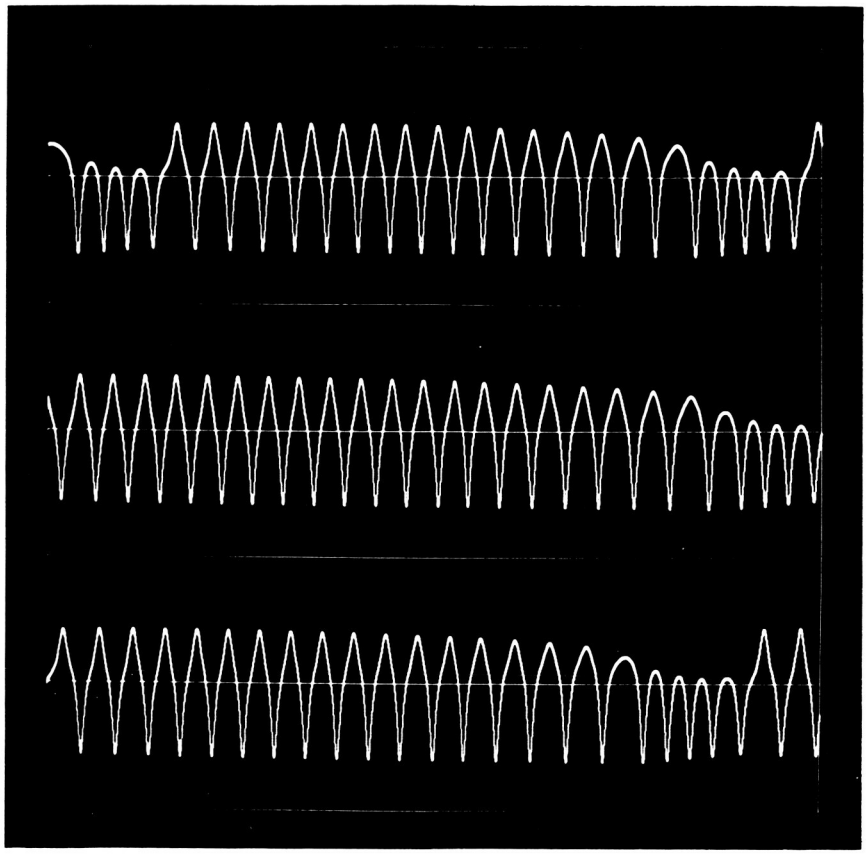

Figure 2. Time integration at R = 1000 and T = 350 showing the irregular modulation.

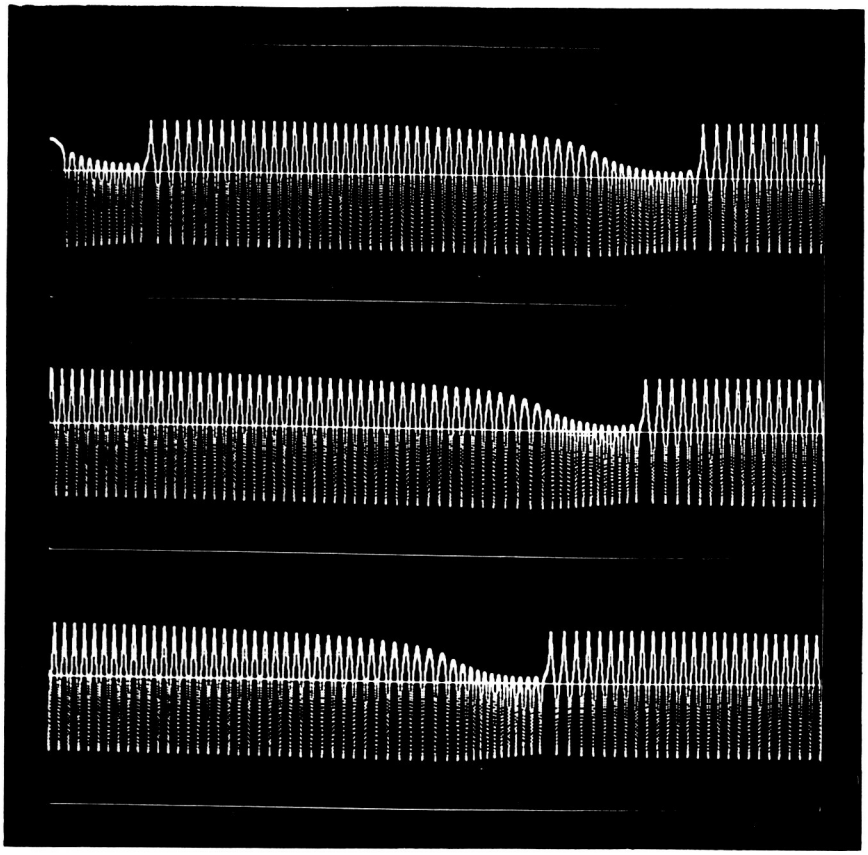

Figure 3. Time integration at R = 10,000 and T = 3500. There are more oscillations in each cycle of the irregular modulation than in Figure 2.

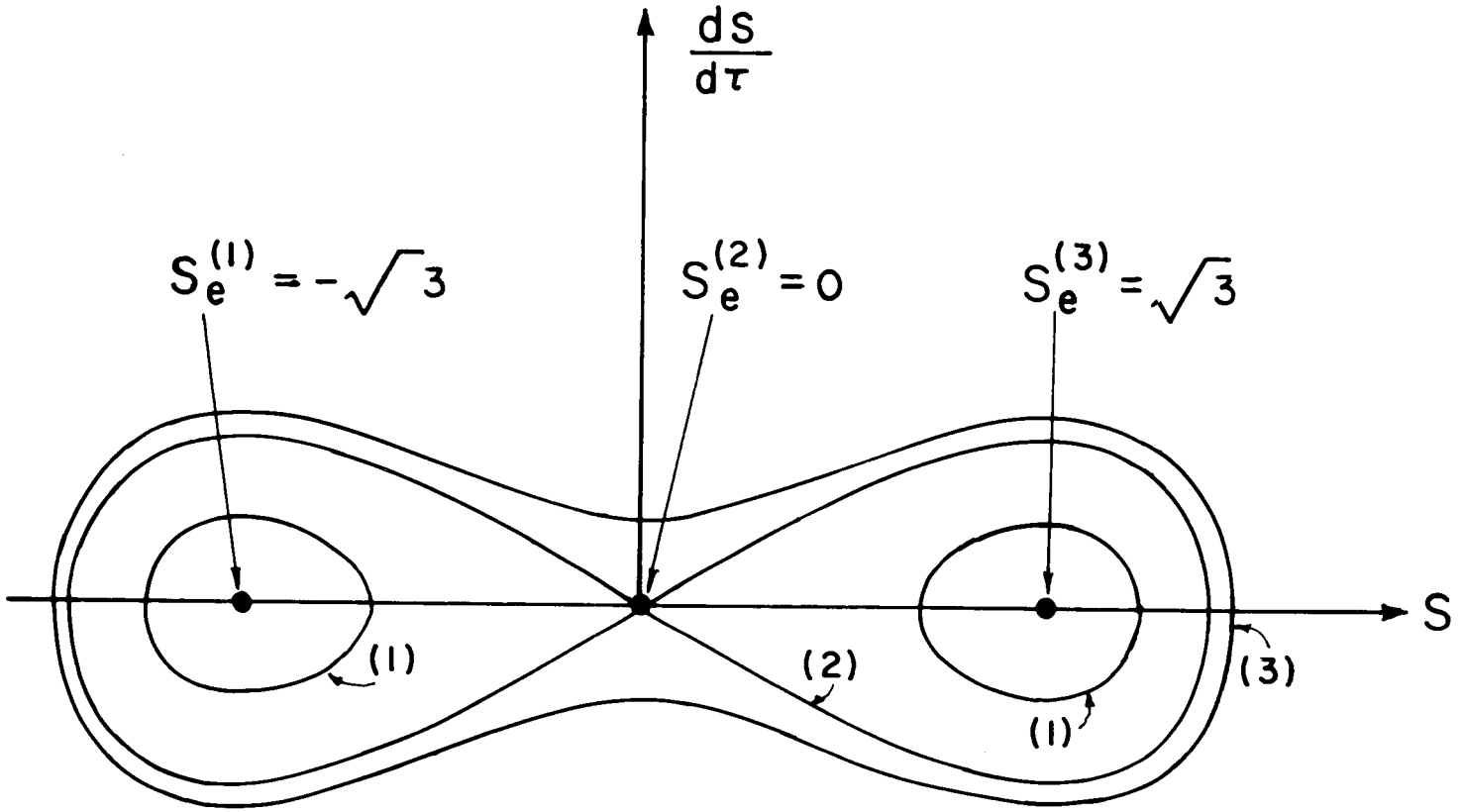

(1) $E^* < 0$

(2 $E^* = 0$ (The Separatrix)

(3) $E^* > 0$

Figure 4a. A sketch of the energy curves for B* = 0

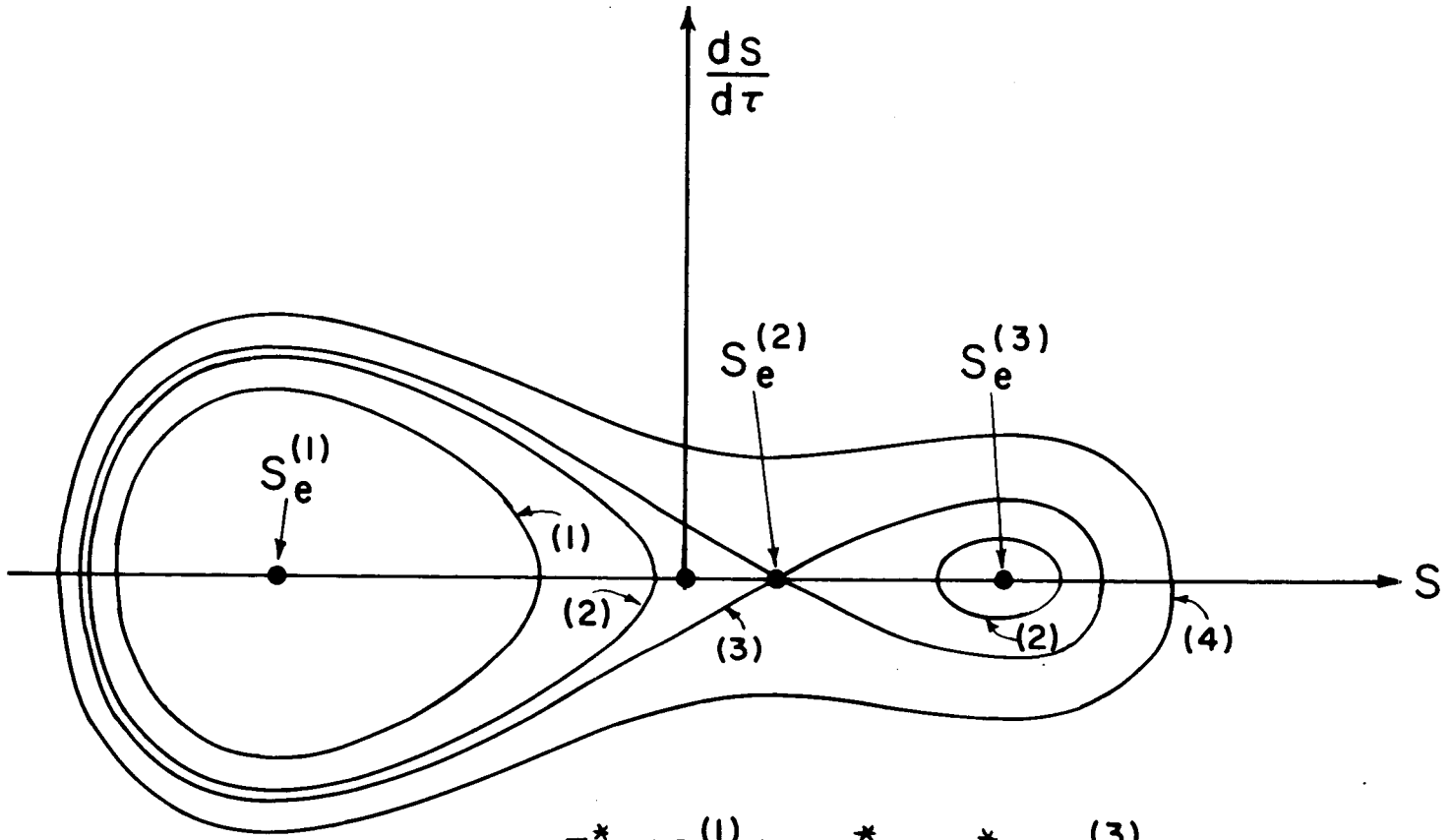

(1) $E^*(S_e^{(1)}) < E^* < E^*(S_e^{(3)})$

(2) $E^*(S_e^{(3)}) < E^* < E^*(S_e^{(2)})$

(3) $E^* = E^*(S_e^{(2)})$ (The Separatrix)

(4) $E^* > E^*(S_e^{(2)})$

Figure 4b. A sketch of the energy curves for $0 < B^* < 2/3$

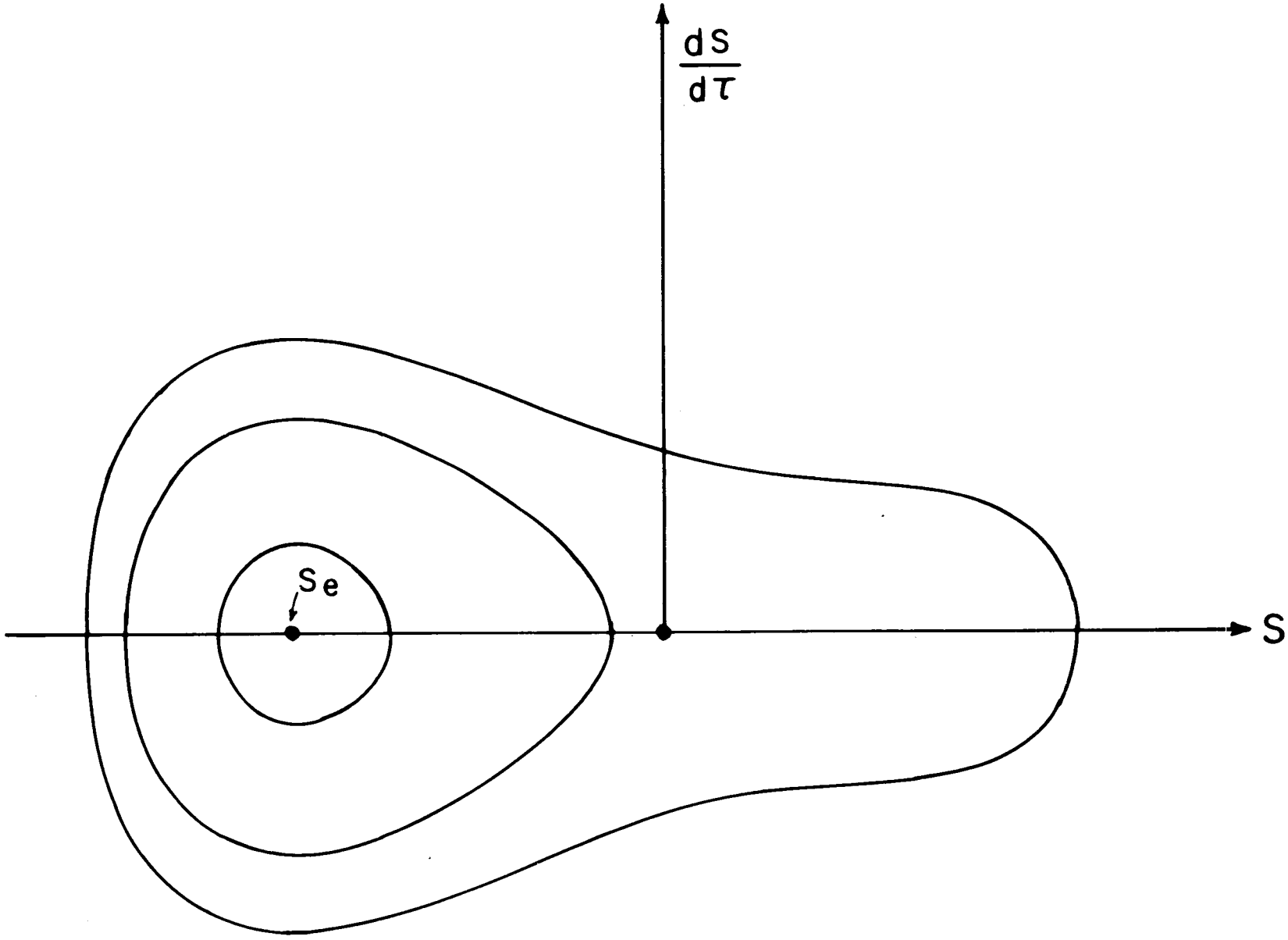

Figure 4c. A sketch of the energy curves for B* > 2/3

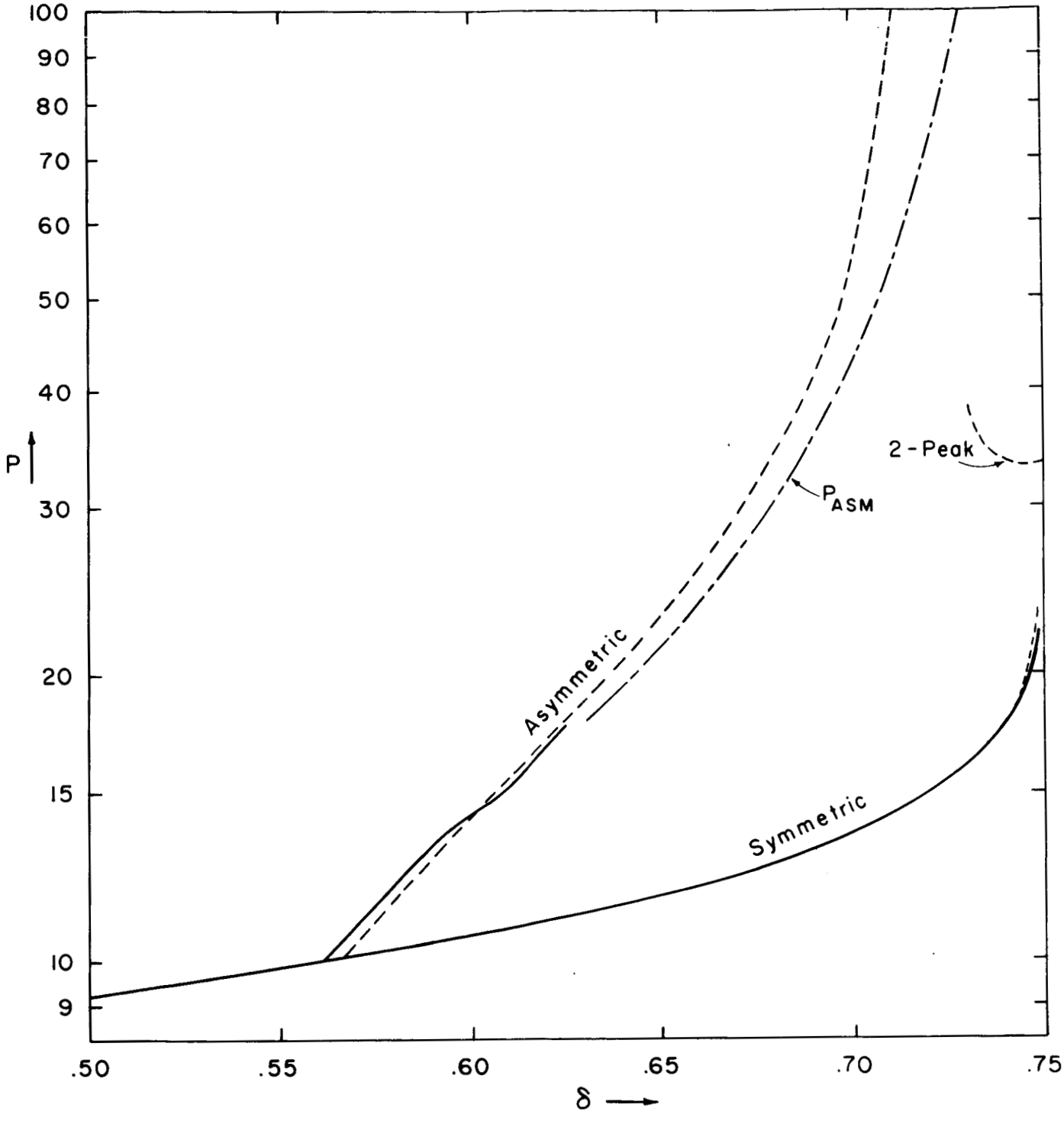

Figure 5. The periods of the symmetric, asymmetric and two-peaked (symmetric) solutions. The period is in dynamical units of time. The solid curves give the periods calculated by the method of averaging; the dashed curves give periods at R = 100 from the numerical relaxation solutions. The values of P_{ASM} from the asymptotic theory valid as $\delta \to 3/4^-$ are shown for comparison.

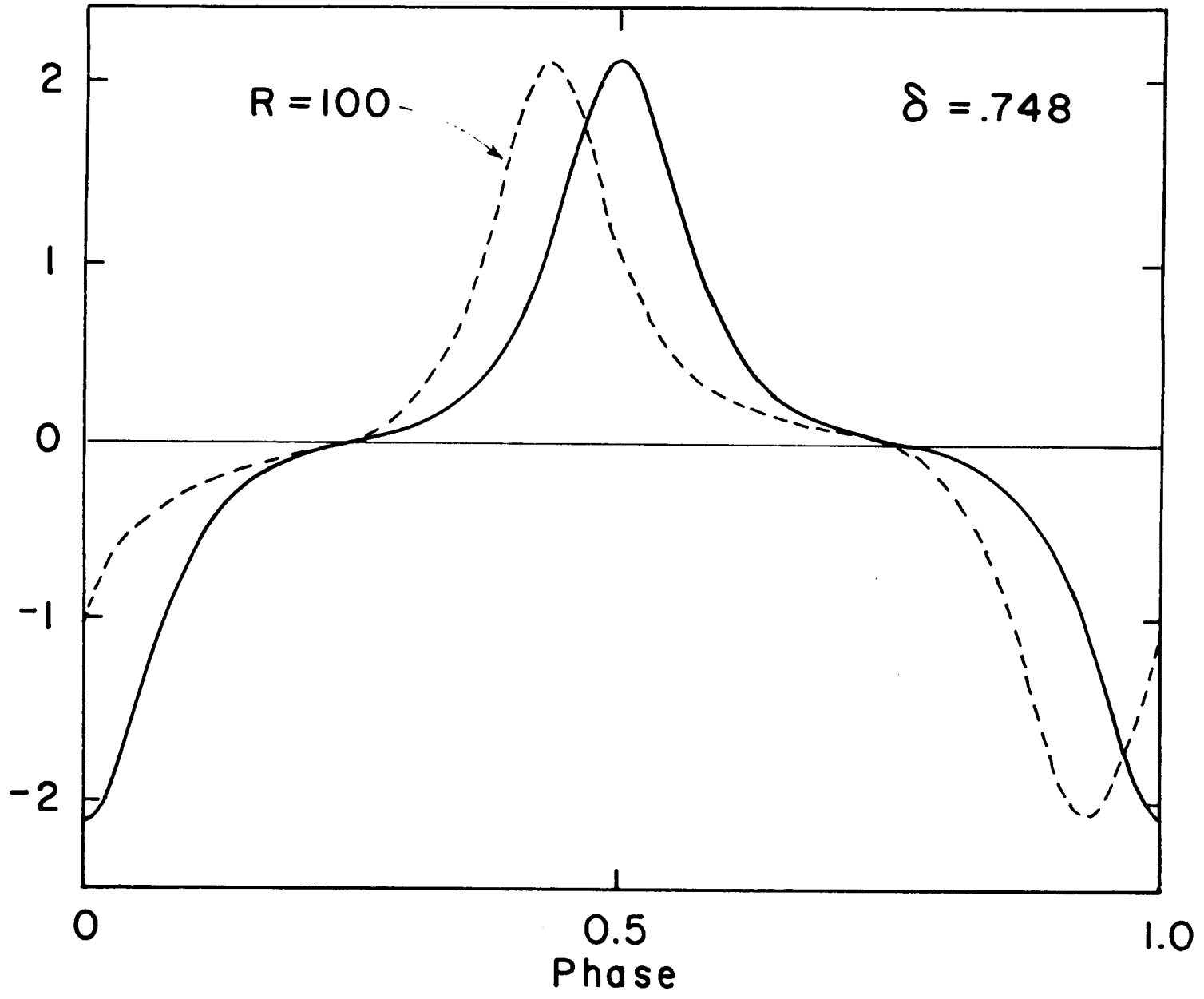

Figure 6. The periodic solution $z_A(\tau)$ given by the method of averaging in the case $\delta = 0.748$ (solid curve). The tendency for long flat portions of small slope and intervening spikes to form as $\delta \to 3/4^-$ is clear. The relaxation solution at $R = 100$, $T = 25.2$, which gives the same δ, is shown for comparison (dashed curve).

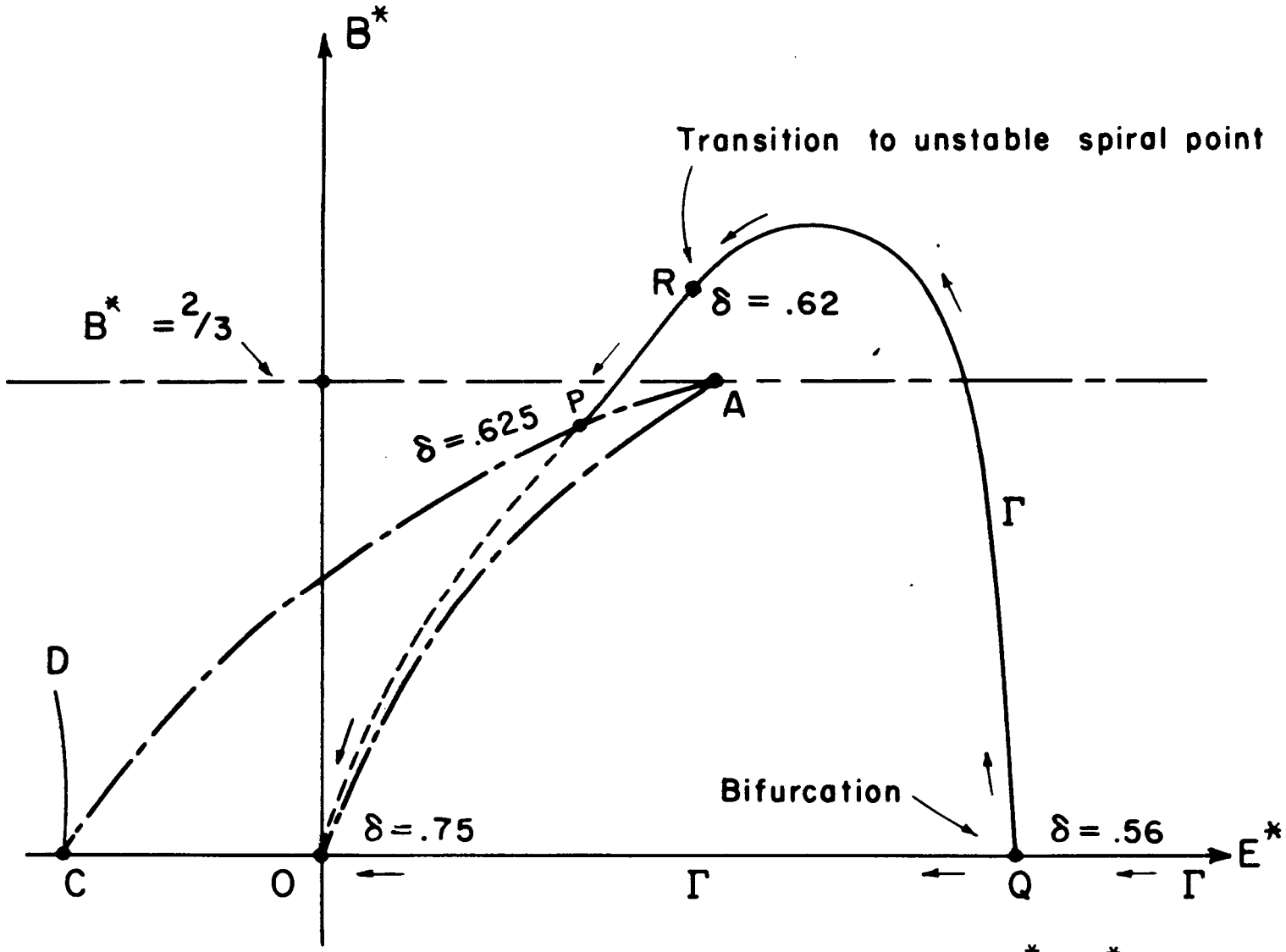

Figure 7. A sketch of the (E*, B*) plane. The locus Γ of values (E_o^*, B_o^*) corresponding to steady periodic solutions is shown. The arrows show the direction δ increasing. To the left of CD there is insufficient energy for any motion. Between CD and CA the energy curve is a single loop surrounding the left-hand equilibrium point. Between CA and OA the energy curve is in two loops, one around each equilibrium. OA corresponds to the separatrix and to the right of OA the energy curve is a single loop surrounding the separatrix.

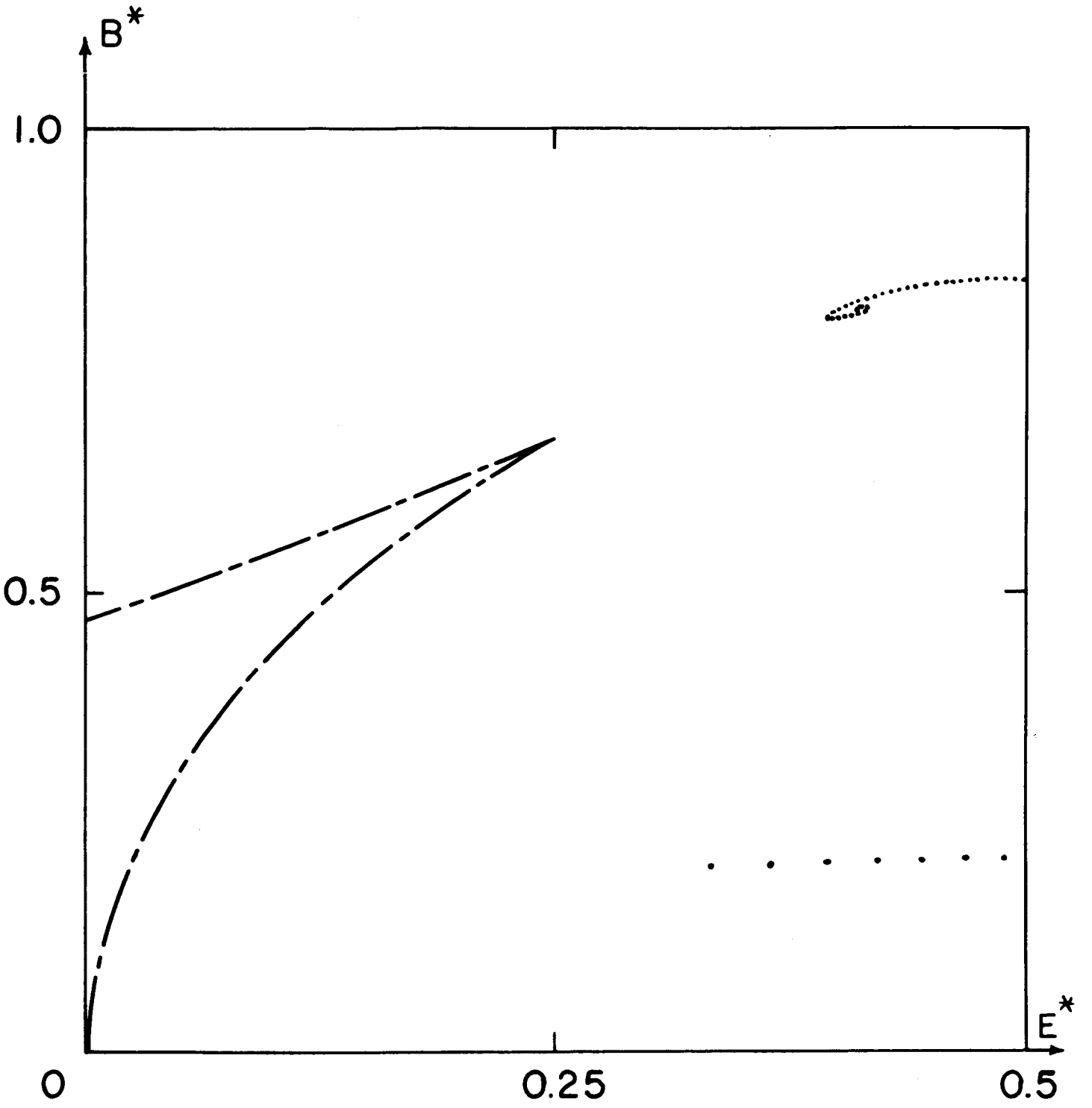

Figure 8a. Time integration of (2.8) for $\delta = 0.6$. The singular point is stable and the solution is spiralling in.

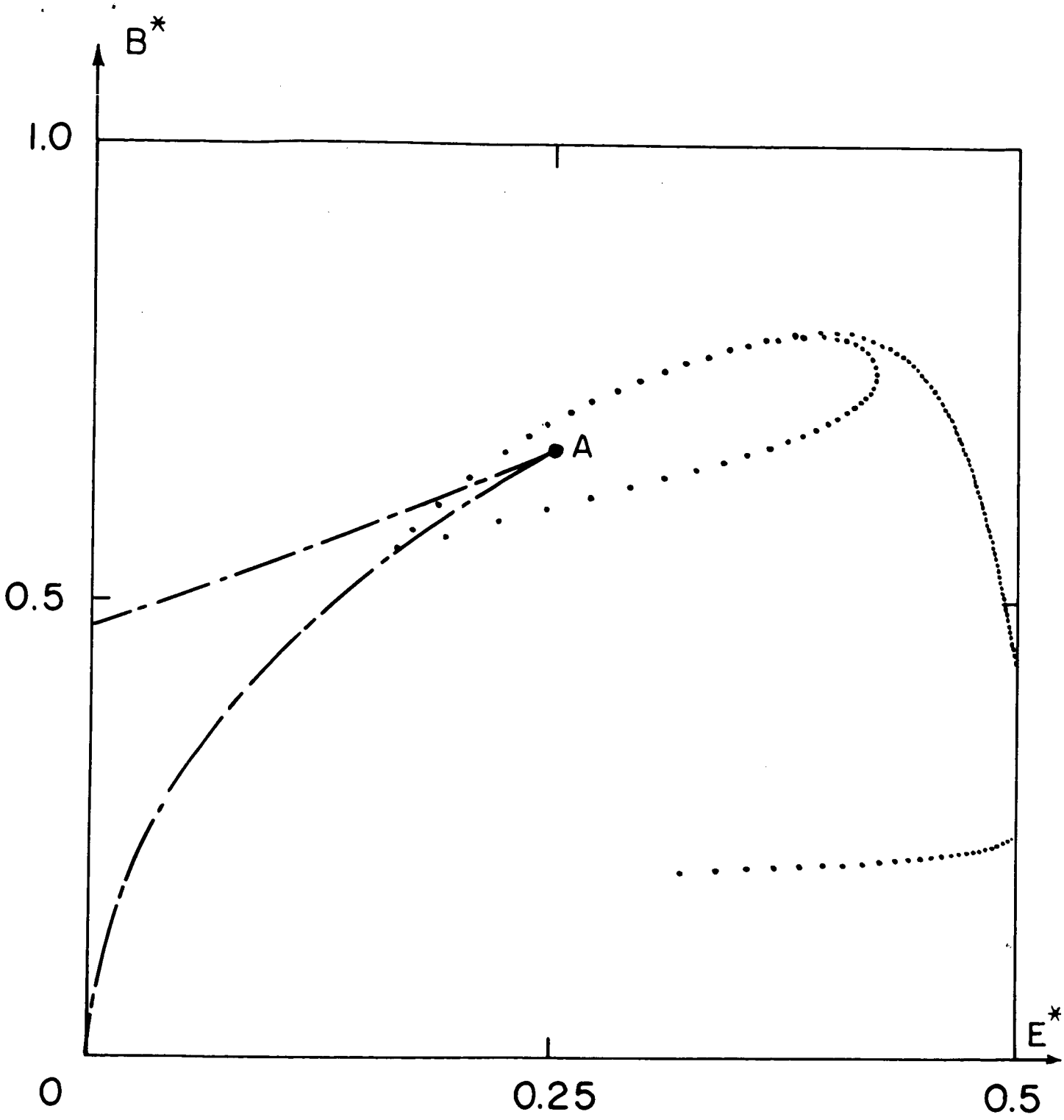

Figure 8b. Time integration of (2.8) for $\delta = 0.625$. The singular point is an unstable spiral and the solution enters a limit cycle. The limit cycle crosses OA from left to right leading to the sudden jump in amplitude of the periodic solution.

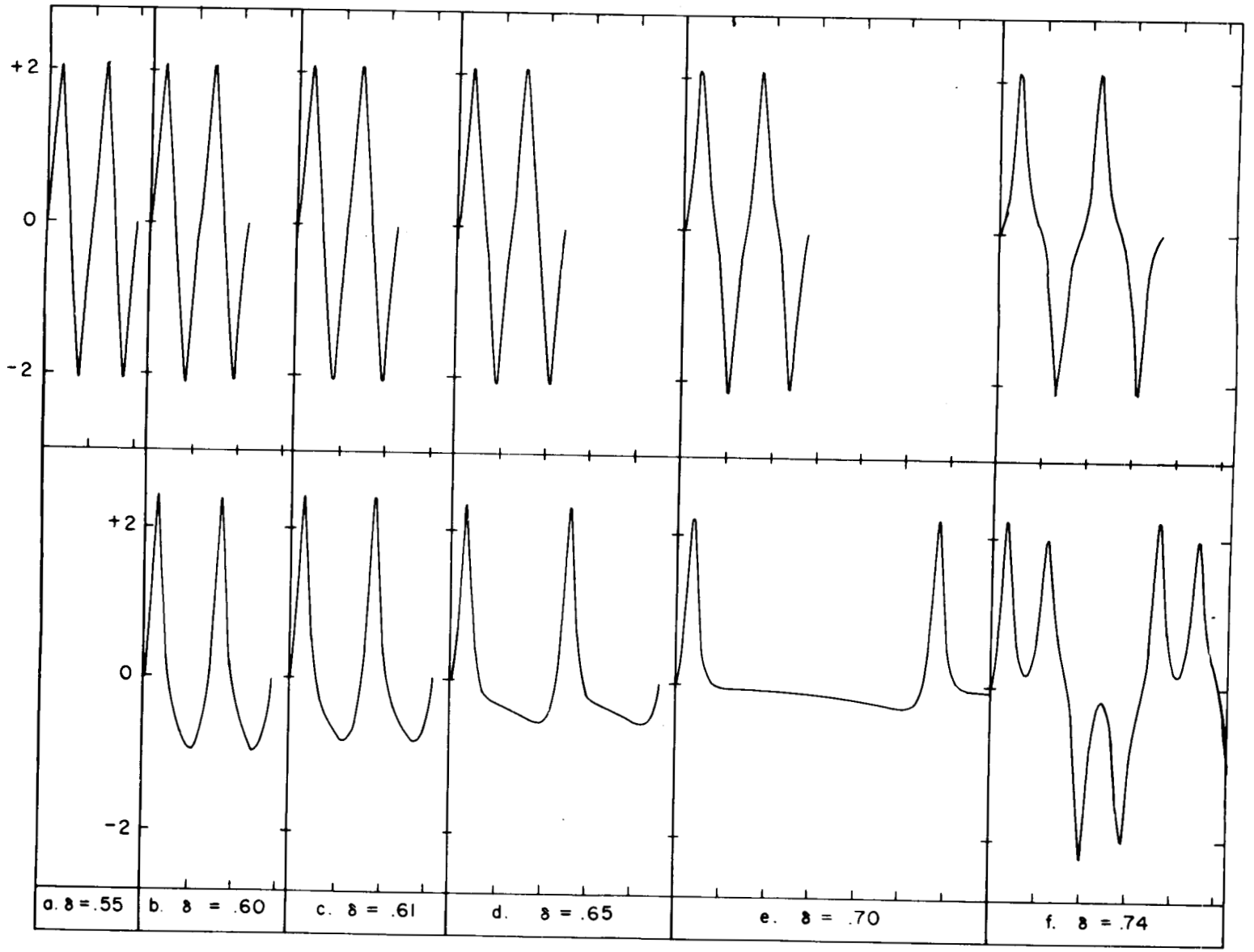

Figure 9. Periodic solutions at R = 100 computed by the relaxation technique for several values of δ. Each division on the horizontal axis is equal to 10 units on the dynamical time scale (which is equal to 1 cooling time at R = 100). The symmetric solution at $\delta = .55$ and the asymmetric solution at $\delta = .60$ are stable; all the other solutions shown are unstable. The asymmetric solution does not exist at $\delta = .55$ but may exist at $\delta = .74$, although it was not found. The 2-peaked solution which was found in the range $.73 < \delta < .75$ is shown at $\delta = .74$.

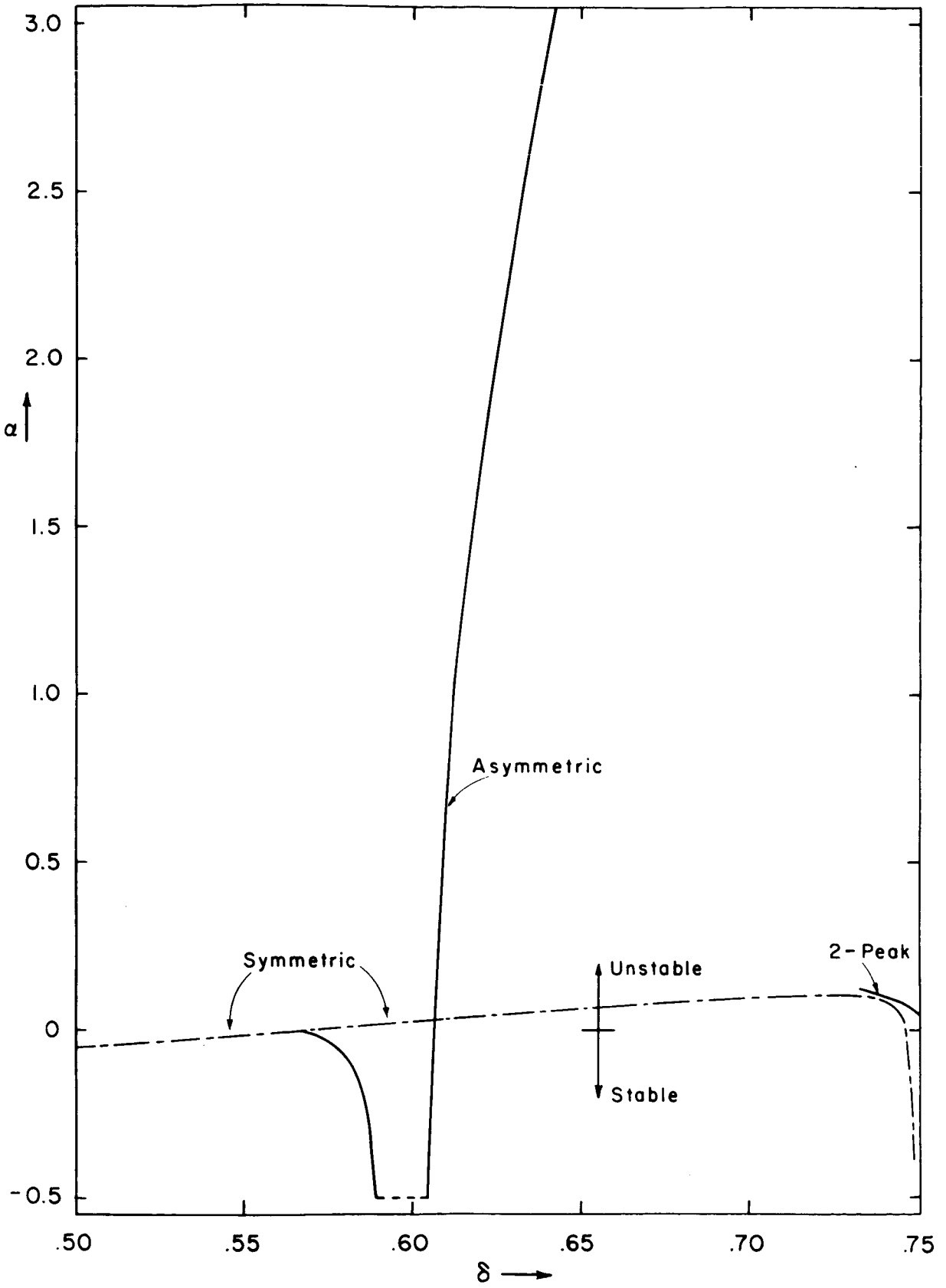

Figure 10. The quantity $\alpha = \lambda^{-1} \ln |\sigma_{MAX}|$, where σ_{MAX} is the Floquet multiplier of greatest modulus, for the symmetric, asymmetric and 2-peaked (symmetric) periodic solutions at R = 100. Negative values of α mean that the corresponding periodic solution is stable; positive values, unstable. The dashed portion of the curve for the asymmetric solution shows the range in which the Floquet multipliers are complex.

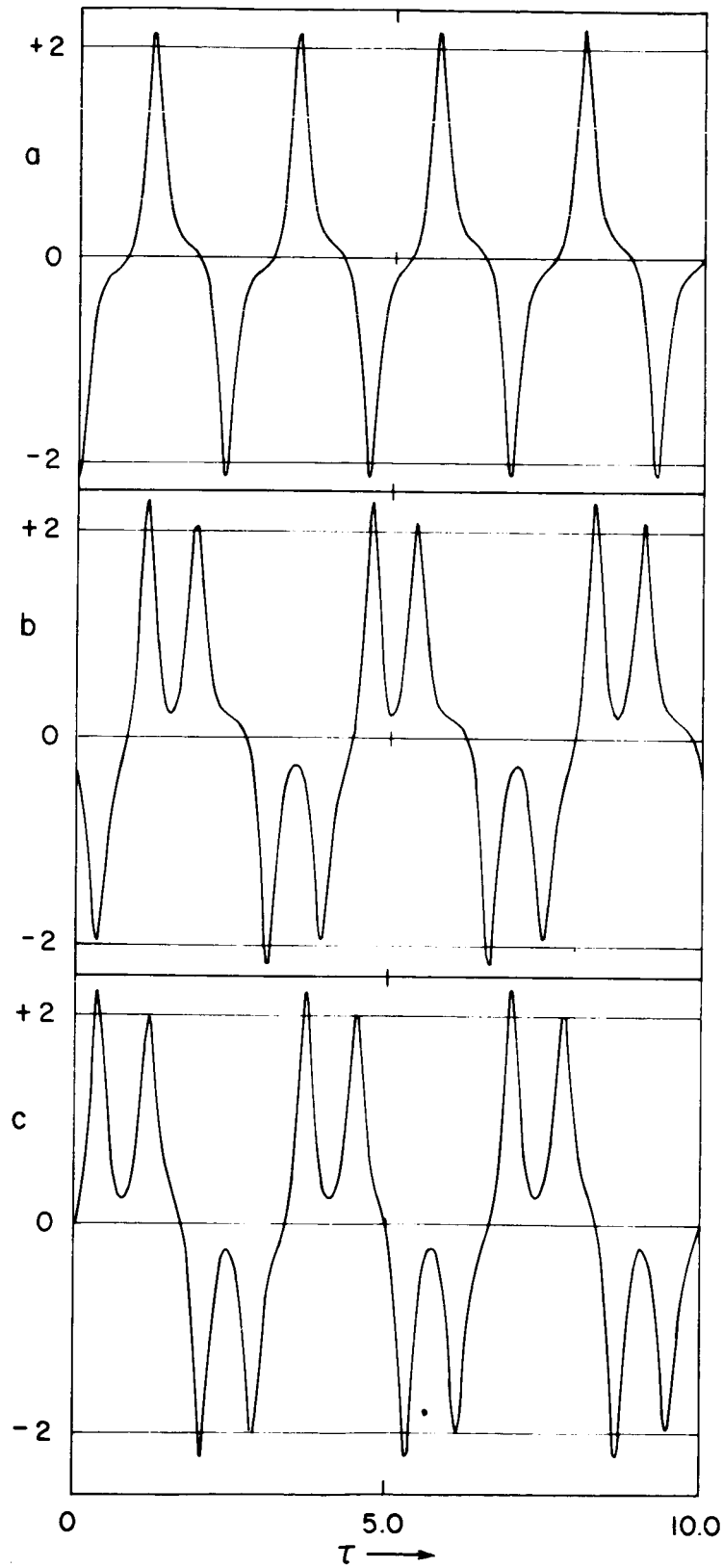

Figure 11. Several periodic solutions found at R = 100, δ = .748. The single-peaked solution (a) and the asymmetric double-peaked solution (b) are stable. The symmetric double-peaked solution (c) is unstable. The time axis is labeled in dynamical units.